

Supplementary Information

Enzymatically Catalyzed Molecular Aggregation

Wen-Jin Wang^{1,2}, Rongyuan Zhang¹, Liping Zhang¹, Liang Hao¹, Xu-Min Cai³, Qian Wu⁴,
Zijie Qiu¹, Ruijuan Han¹, Jing Feng¹, Shaojuan Wang^{1*}, Parvej Alam¹, Guoqing Zhang²,
Zheng Zhao^{1*} and Ben Zhong Tang^{1,4*}

¹ Clinical Translational Research Center of Aggregation-Induced Emission, The Second Affiliated Hospital, School of Medicine, School of Science and Engineering Shenzhen Institute of Aggregate Science and Technology, The Chinese University of Hong Kong, Shenzhen (CUHK-Shenzhen), Guangdong 518172, China

² University of Science and Technology of China, Hefei, Anhui 230026, China

³ Jiangsu Co-Innovation Center of Efficient Processing and Utilization of Forest Resources International Innovation Center for Forest Chemicals and Materials College of Chemical Engineering Nanjing Forestry University

⁴ Department of Chemistry, Hong Kong Branch of Chinese National Engineering Research Center for Tissue Restoration and Reconstruction, Institute of Molecular Functional Materials, Division of Life Science and State Key Laboratory of Molecular Neuroscience, The Hong Kong University of Science and Technology, Clear Water Bay, Kowloon, Hong Kong, China

* Corresponding authors. Email: 609199354@qq.com (S. W.), zhaozheng@cuhk.edu.cn (Z. Z), tangbenz@cuhk.edu.cn (B. Z. T)

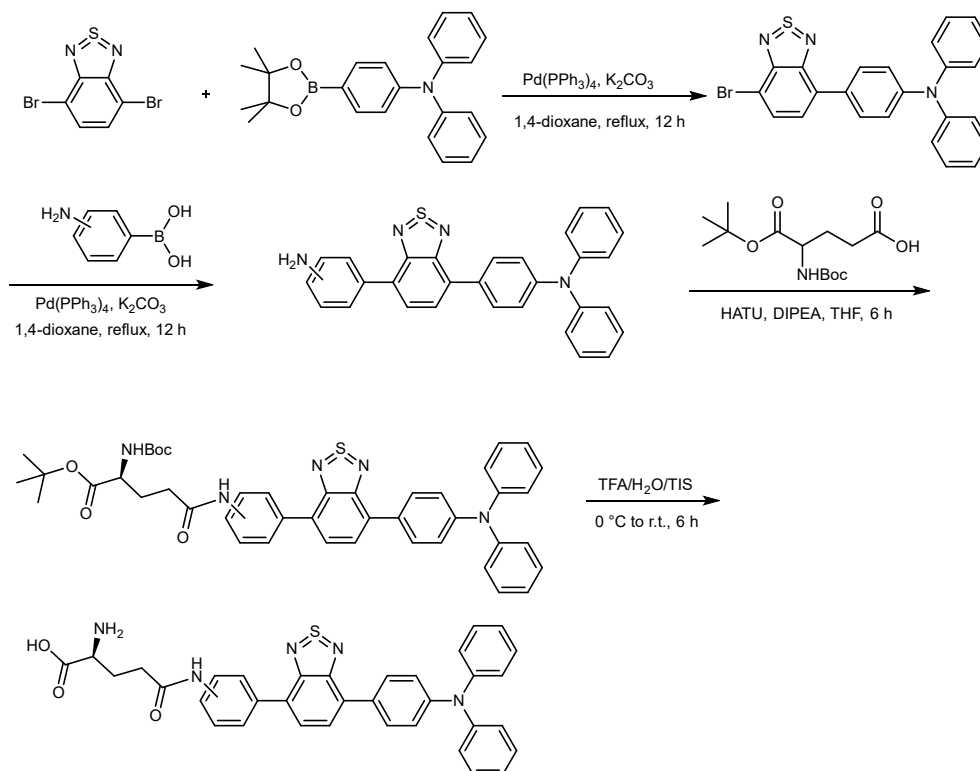
Experimental Section

General

Materials: 4, 7-dibromo-2,1, 3-benzothiadiazole, N-(4-(4,4,5,5-Tetramethyl-1,3,2-dioxaborolan-2-yl)phenyl)-N-phenylbenzenamine were purchased from Energy Chemical, China. Tetratriphenylphosphine palladium, 2-(7-Azabenzotriazol-1-yl)-N,N,N',N'-tetramethyluronium hexafluorophosphate (HATU) were purchased from Adamas-beta (China). N,N-Diisopropylethylamine, 3-aminobenylboric acid, and 4-aminobenylboric acid were obtained from Didepharm (China). Dimethyl sulfoxide (DMSO), 2',7'-Dichlorodihydrofluorescein diacetate (H₂DCF-DA), Hydroxyphenyl fluorescein (HPF), 9,10-Anthracenediyl-bis(methylene)dimalonic Acid (ABDA), Glutamyltransferase (G9270) and 3-(4,5-dimethyl-2-thiazolyl)-2,5-diphenyl-2-H-tetrazolium bromide (MTT) were purchased from Sigma–Aldrich. Dulbecco's modified eagle medium (DMEM, Giobic®), Roswell Park Memorial Institute medium (RPMI1640 Medium, Giobic®), fetal bovine serum (FBS, Giobic®), trypsin (Giobic®), Phosphate-Buffered Saline (PBS, Giobic®), penicillin-streptomycin solution (Giobic®) were brought from ThermoFisher Scientific. The antibodies for GGT (ab109427), GPX4 (ab125066), and β -actin (ab8226) were obtained from Abcam. All the other reagents were obtained through commercial resources. All the tested compounds were dissolved in DMSO as stock solution and diluted into the expected experiment concentration containing 1% (v/v) DMSO as needed.

General instruments: ESI-MS was carried out on a Thermo Scientific LTQ linear ion trap mass spectrometer. ¹H NMR and ¹³C NMR were recorded by a Bruker AVANCE III 500 MHz spectrometer (Germany). Chemical shifts were referenced relative to the internal solvent signals. Fluorescence measurements were conducted on an FLS1000 system (Edinburgh Instruments) and Horiba PL spectrometer (Fluorolog-3). High-resolution mass spectra (HRMS) were collected on a Bruker maXis ultra-high resolution (UHR)-TOF mass spectrometer in electrospray ionization (ESI)-positive mode. Cell viability was measured using a Molecular Devices FlexStation 3 microplate reader (USA). Cell imaging assays were performed on a Leica TCS SP8 STED 3X confocal laser scanning fluorescence microscopy and Leica DMi8 inversion microscope (Germany). Flow cytometry was conducted on a BD FACS Calibur (USA).

Synthesis and characterization



Supplementary Fig. 1. The synthetic route for TBmA-Glu and TBpA-Glu.

4-(7-bromobenzo[*c*][1,2,5]thiadiazol-4-yl)-N,N-diphenylaniline (3): Compound **3** was synthesized according to the reported method¹ with minor modification: 4, 7-dibromo-2,1, 3-benzothiadiazole (**1**, 587.9 mg, 2.0 mmol), N-(4-(4,4,5,5-Tetramethyl-1,3,2-dioxaborolan-2-yl)phenyl)-N-phenylbenzenamine (**2**, 891.1 mg, 2.4 mmol) were added to 100 mL round-bottomed flask along with potassium carbonate (829.3 mg, 6 mmol) and tetratriphenylphosphine palladium (69.3 mg, 0.06 mmol) in 40 mL of 1, 4-dioxane. The mixture was refluxed under N₂ for 12 h. After the reaction was finished, the catalyst was removed by filtration, and the solvent was removed under reduced pressure. The concentrated liquid was dissolved in methylene chloride (CH₂Cl₂) and washed using a brine solution (NaCl). The organic layer was dried using anhydrous sodium sulfate, concentrated, and finally purified by column chromatography (PE: EA=5:1) to obtain orange-red powder **3** with a yield of 73.2%. The structure of **3** was characterized and confirmed through ¹H NMR and HR-ESI-MS, which are coordinated with the reported data.

4-(7-(3-aminophenyl)benzo[c][1,2,5]thiadiazol-4-yl)-N,N-diphenylaniline (TBmA, 4a): The product **2** (475.0 mg, 1 mmol) and 3-aminobenzylboric acid (178.0 mg, 1.3 mmol) were added into a 50 mL round-bottomed flask, respectively. Potassium carbonate (414.7 mg, 3 mmol) and tetratriphenylphosphine palladium (34.7 mg, 0.03 mmol) were dissolved in 20 mL of 1, 4-dioxane. Reflux reaction under argon protection overnight. After the reaction, the catalyst was removed by filtration, and the solvent was removed under reduced pressure. The concentrated liquid was dissolved in methylene chloride (CH₂Cl₂) and washed using a brine solution (NaCl). The organic layer was dried using anhydrous sodium sulfate, concentrated, and finally purified by column chromatography (PE: EA=3:1) to obtain a red powder of TBmA with a yield of 56%. ¹H NMR (500 MHz, CDCl₃) δ (ppm): 7.87 (d, *J* = 8.2 Hz, 2H), 7.74 (s, 2H), 7.38 – 7.26 (m, 8H), 7.20 (t, *J* = 9.3 Hz, 7H), 7.07 (t, *J* = 7.4 Hz, 2H), 6.83 (d, *J* = 6.8 Hz, 1H). ¹³C NMR (125 MHz, CDCl₃) δ (ppm) 154.36, 148.38, 147.80, 138.96, 133.12, 131.24, 130.27, 129.90, 129.70, 128.54, 127.61, 125.25, 123.65, 123.22, 120.45, 116.59. HR-ESI-MS (CH₃OH) *m/z*: calculated for [M+H]⁺ (C₃₀H₂₃N₄S⁺) 471.1643, found 471.1638.

4-(7-(4-aminophenyl)benzo[c][1,2,5]thiadiazol-4-yl)-N,N-diphenylaniline (TBpA, 4b): TBpA was prepared via the similar synthetic method as TBmA with 4-aminobenzylboric acid instead of 3-aminobenzylboric acid. TBpA was obtained as a red powder with a yield of 65.4%. ¹H NMR (500 MHz, DMSO-*d*₆) δ (ppm): 7.94 (d, *J* = 8.3 Hz, 2H), 7.82 (dd, *J* = 22.7, 8.2 Hz, 4H), 7.35 (t, *J* = 7.8 Hz, 4H), 7.10 (d, *J* = 7.8 Hz, 8H), 6.72 (d, *J* = 8.2 Hz, 2H), 5.45 (s, 2H). ¹³C NMR (125 MHz, DMSO-*d*₆) δ (ppm): 153.63, 153.58, 149.32, 147.18, 147.03, 132.45, 130.97, 130.05, 129.97, 129.74, 127.81, 125.92, 124.43, 123.50, 122.62, 113.77. HR-ESI-MS (CH₃OH) *m/z*: calculated for [M+H]⁺ (C₃₀H₂₃N₄S⁺) 471.1643, found 471.1664.

Tert-butyl **N2-(tert-butoxycarbonyl)-N5-(3-(7-(4-(diphenylamino)phenyl)benzo[c][1,2,5]thiadiazol-4-yl)phenyl)-L-glutamate (5a)** and

tert-butyl **N2-(tert-butoxycarbonyl)-N5-(4-(7-(4-(diphenylamino)phenyl)benzo[c][1,2,5]thiadiazol-4-yl)phenyl)-L-glutamate (5b):**

TBmA or TBpA (235.3 mg, 0.5 mmol), Boc-L-glutamate-1-tert-butyl ester (227.5 mg, 0.75 mmol) were added to 50 mL round-bottled flask, respectively. HATU (384.2 mg, 1 mmol) and DIPEA (193.9 mg, 1.5 mmol) were dissolved in 10 mL tetrahydrofuran and reacted overnight at room temperature. After the reaction, it was washed with saturated salt water, extracted using methylene chloride, dried using anhydrous sodium sulfate, and purified by column chromatography (PE: EA=1:1) to obtain target products.

5a: orange powder (yield 92.3%). ¹H NMR (500 MHz, DMSO-*d*₆) δ (ppm): 10.07 (s, 1H), 8.24 (s, 1H), 7.98 (d, *J* = 8.3 Hz, 2H), 7.94 (d, *J* = 7.4 Hz, 1H), 7.88 (d, *J* = 7.4 Hz, 1H), 7.67 (dd, *J* = 16.8, 7.9 Hz, 2H), 7.47 (t, *J* = 7.9 Hz, 1H), 7.37 (t, *J* = 7.7 Hz, 4H), 7.15 – 7.05 (m, 8H), 3.87 (q, *J* = 8.0 Hz, 1H), 2.49 – 2.41 (m, 3H), 2.05 – 1.97 (m, 1H), 1.83 (dd, *J* = 14.5, 8.1 Hz, 1H), 1.41 (s, 18H). ¹³C NMR (125 MHz, DMSO-*d*₆) δ (ppm): 171.62, 170.51, 155.53, 153.39, 153.34, 147.48, 146.87, 139.44, 137.33, 131.85, 131.63, 130.38, 130.17, 129.67, 128.86, 128.38, 127.39, 124.49, 123.84, 123.55, 122.29, 119.68, 118.91, 80.33, 78.06, 53.88, 32.69, 28.18, 27.66, 26.19. HR-ESI-MS (CH₃OH) *m/z*: calculated for [M+H]⁺ (C₄₄H₄₆N₅O₅S⁺) 756.3241, found 756.3234.

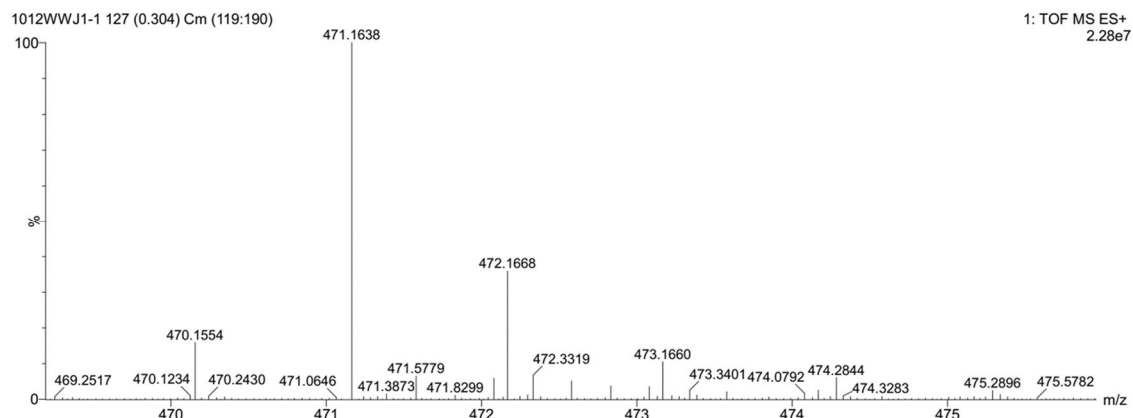
5b: red powder (yield 90.6%). ¹H NMR (500 MHz, DMSO-*d*₆) δ (ppm): 10.11 (s, 1H), 7.98 (dd, *J* = 15.1, 8.3 Hz, 4H), 7.91 (s, 2H), 7.77 (d, *J* = 8.3 Hz, 2H), 7.36 (t, *J* = 7.8 Hz, 4H), 7.20 (d, *J* = 7.9 Hz, 1H), 7.12 (d, *J* = 7.8 Hz, 7H), 3.87 (q, *J* = 7.8 Hz, 1H), 2.46 (t, *J* = 7.7 Hz, 3H), 2.06 – 2.02 (m, 1H), 1.83 (dd, *J* = 14.6, 8.1 Hz, 1H), 1.42 (s, 18H). ¹³C NMR (125 MHz, DMSO-*d*₆) δ (ppm): 171.62, 170.52, 155.54, 153.40, 147.38, 146.88, 139.36, 131.35, 131.24, 130.50, 130.10, 129.67, 129.40, 127.66, 127.46, 124.46, 123.52, 122.33, 118.89, 80.34, 78.07, 53.88, 32.73, 28.20, 27.94, 27.67, 26.17. HR-ESI-MS (CH₃OH) *m/z*: calculated for [M+Na]⁺ (C₄₄H₄₆N₅O₅S⁺) 778.3034, found 778.3057.

N5-(3-(7-(4-(diphenylamino)phenyl)benzo[c][1,2,5]thiadiazol-4-yl)phenyl)-L-glutamine (TBmA-Glu, 6a) and **N5-(4-(7-(4-(diphenylamino)phenyl)benzo[c][1,2,5]thiadiazol-4-**

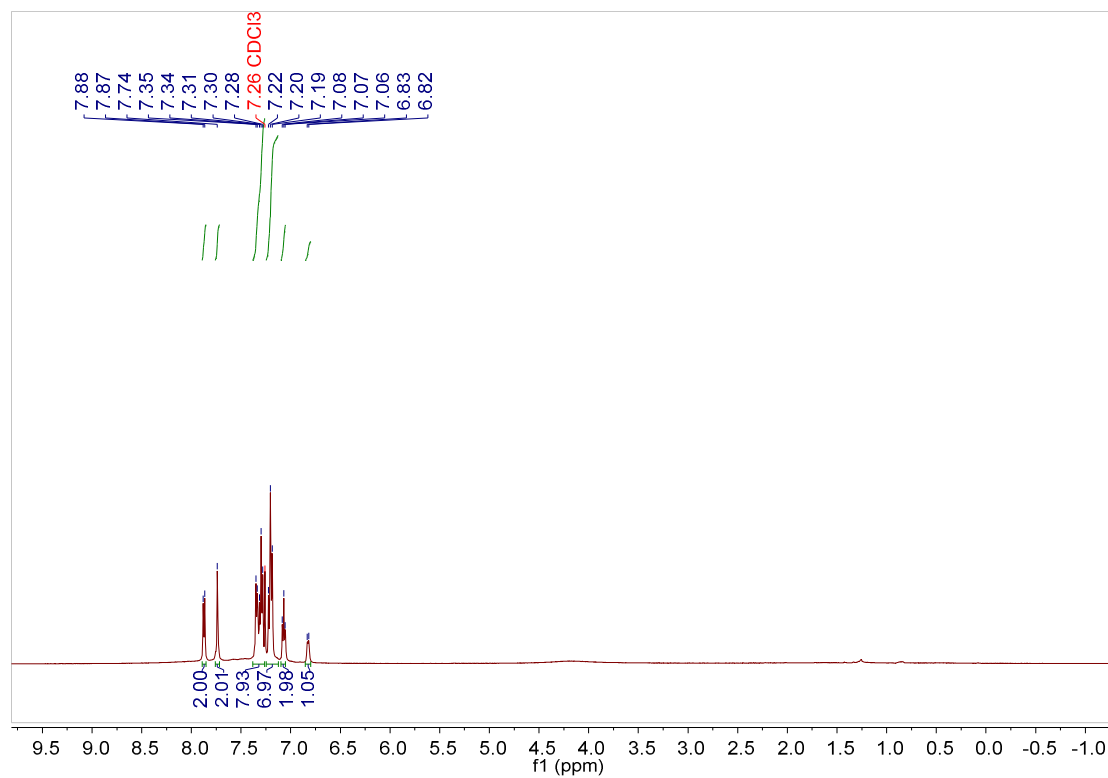
yl)phenyl)-L-glutamine (TBpA-Glu, 6b): The (270 mg, 0.2 mmol) obtained in the previous step was added to a 25 mL round-bottomed flask, and a mixture of 5 mL trifluoroacetic acid/water/triisopropyl silane was added drop by drop under ice bath cooling ($V_{\text{TFA}}/V_{\text{H}_2\text{O}}/V_{\text{TIS}}=95:2.5:2.5$). The reaction was heated to room temperature for 10 min and continued for 5 h. After the reaction, the solvent was removed under reduced pressure, and the solid obtained was recrystallized with ethyl acetate to obtain glutamic acid-modified AIE-PS, TBmA-Glu: red powder (yield 98.4%). ^1H NMR (500 MHz, DMSO- d_6) δ (ppm): 10.55 (s, 1H), 8.26 (s, 1H), 7.93 (dd, $J = 20.0, 7.9$ Hz, 5H), 7.85 (d, $J = 7.5$ Hz, 1H), 7.73 (d, $J = 8.1$ Hz, 1H), 7.64 (d, $J = 7.8$ Hz, 1H), 7.45 (t, $J = 8.0$ Hz, 1H), 7.36 (t, $J = 7.8$ Hz, 4H), 7.14 – 7.07 (m, 8H), 2.59 (d, $J = 8.1$ Hz, 2H), 2.15 – 2.04 (m, 2H), 2.02 (s, 1H). ^{13}C NMR (125 MHz, DMSO- d_6) δ (ppm): 153.41, 147.49, 146.88, 139.53, 137.33, 131.85, 131.67, 130.39, 130.19, 129.71, 128.83, 128.40, 127.40, 124.51, 123.59, 122.29, 119.75, 119.02, 59.78, 53.39, 32.81, 14.11. HR-ESI-MS (CH₃OH) m/z : calculated for $[\text{M}+\text{H}]^+$ (C₃₅H₃₀N₅O₃S⁺) 600.2064, found 600.2089.

TBpA-Glu: red powder (yield 98.2%). ^1H NMR (500 MHz, DMSO- d_6) δ (ppm): 10.41 (s, 1H), 7.97 (dd, $J = 12.9, 6.7$ Hz, 4H), 7.88 (s, 2H), 7.78 (d, $J = 6.5$ Hz, 2H), 7.36 (t, $J = 6.3$ Hz, 4H), 7.11 (dd, $J = 6.7, 3.7$ Hz, 8H), 3.67 – 3.58 (m, 1H), 2.63 – 2.55 (m, 2H), 2.06 (m, 2H). ^{13}C NMR (125 MHz, DMSO) δ 170.33, 153.29, 146.77, 130.01, 129.58, 129.31, 127.58, 127.34, 124.36, 123.45, 122.21, 118.89, 59.64, 20.66, 13.98. HR-ESI-MS (CH₃OH) m/z : calculated for $[\text{M}+\text{H}]^+$ (C₃₅H₃₀N₅O₃S⁺) 600.2064, found 600.2072.

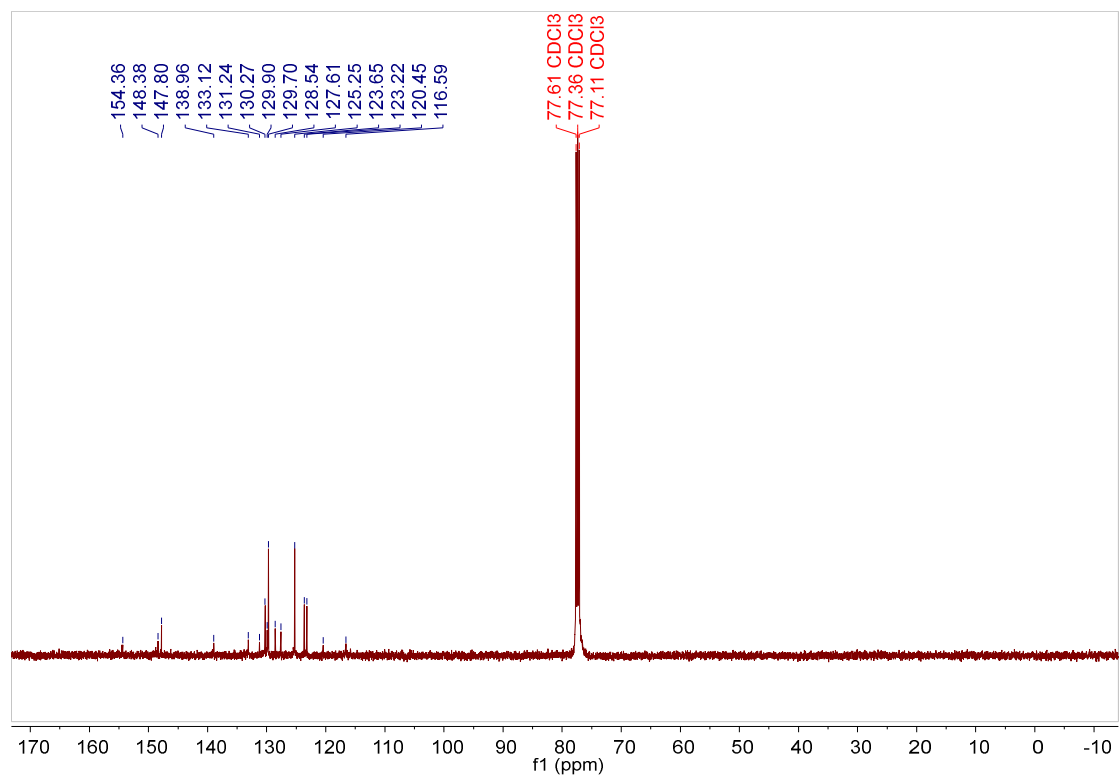
Supplementary Figures



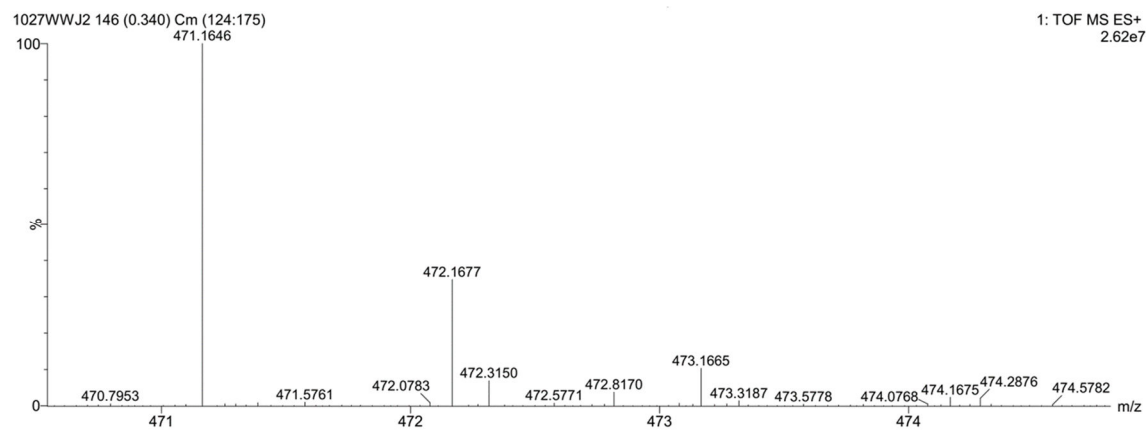
Supplementary Fig. 2. HRMS of TBmA.



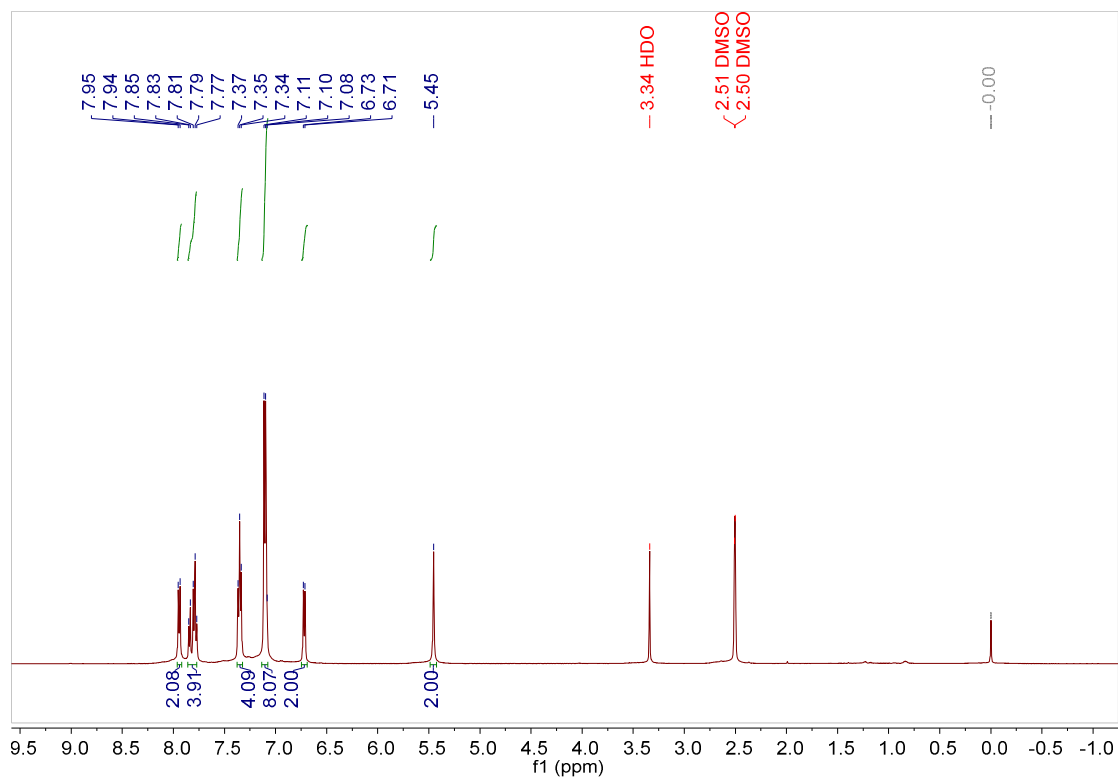
Supplementary Fig. 3. ¹H NMR spectrum of TBmA.



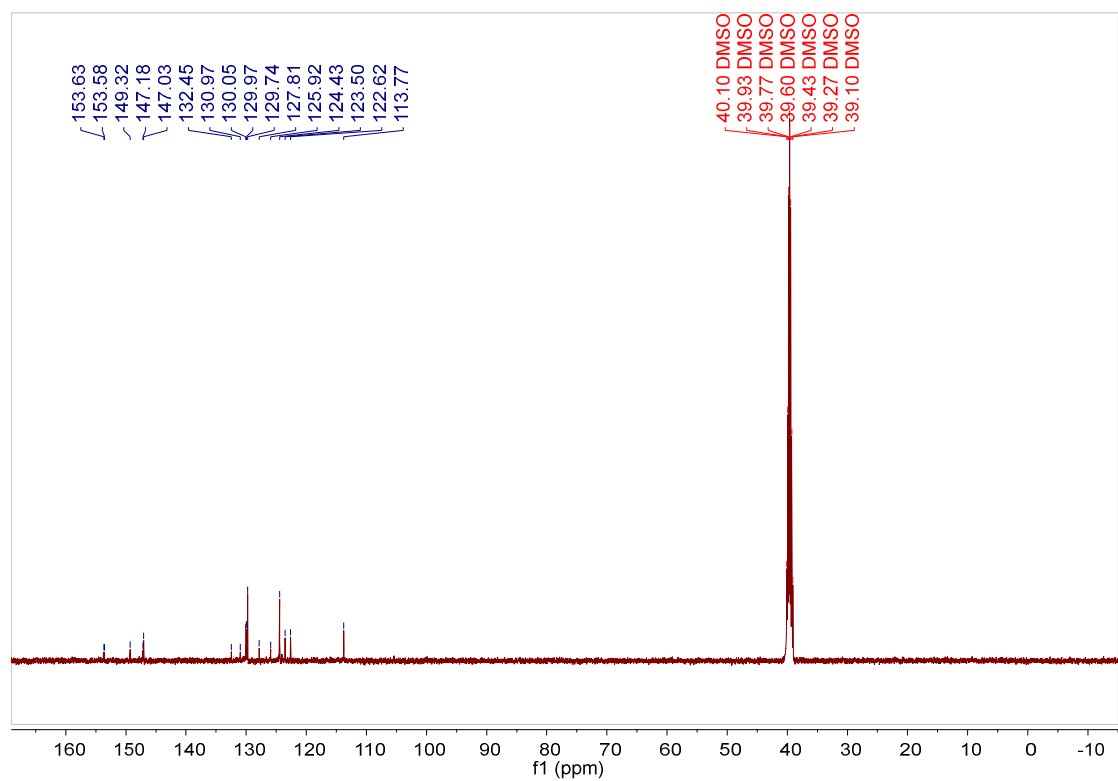
Supplementary Fig. 4. ¹³C NMR spectrum of TBmA.



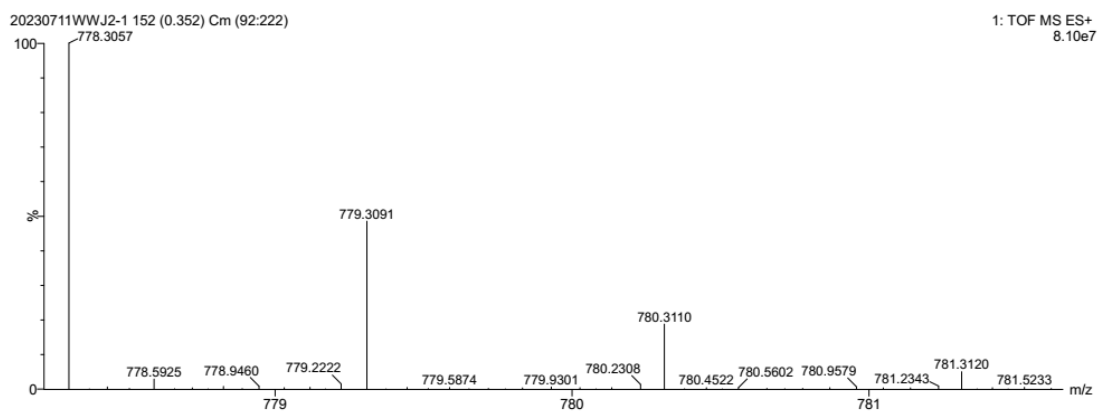
Supplementary Fig. 5. HRMS spectrum of TBpA.



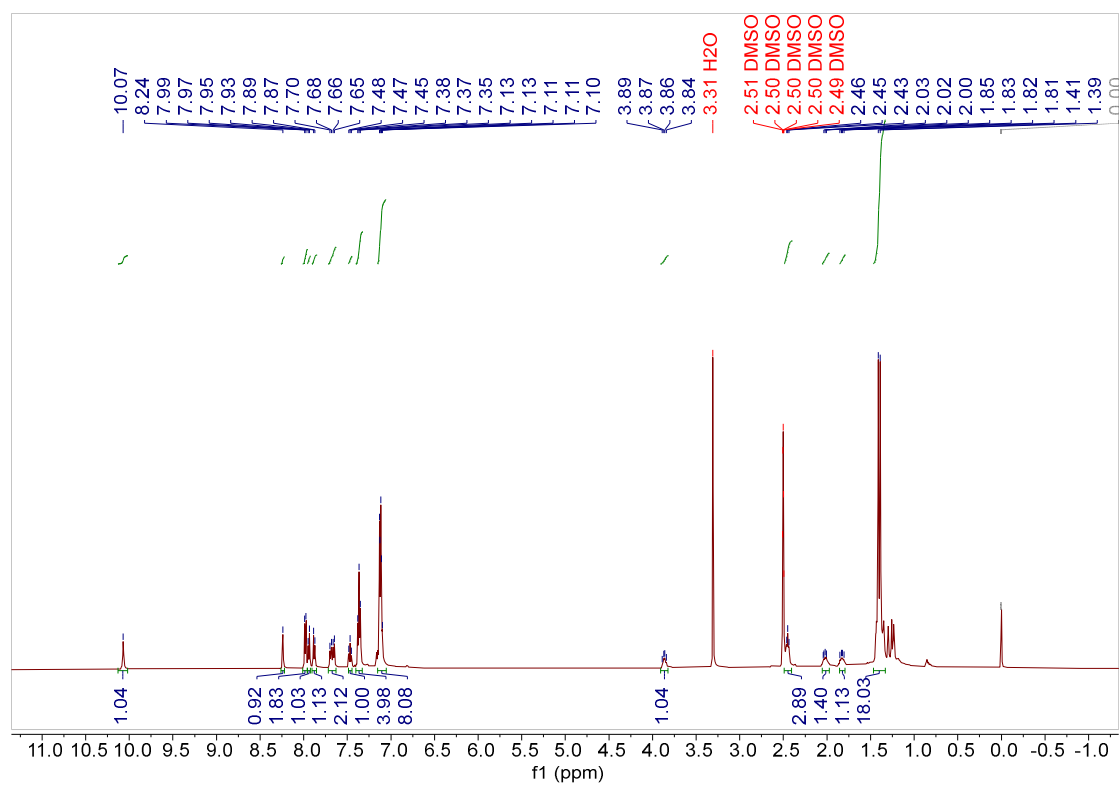
Supplementary Fig. 6. ¹H NMR spectrum of TBpA.



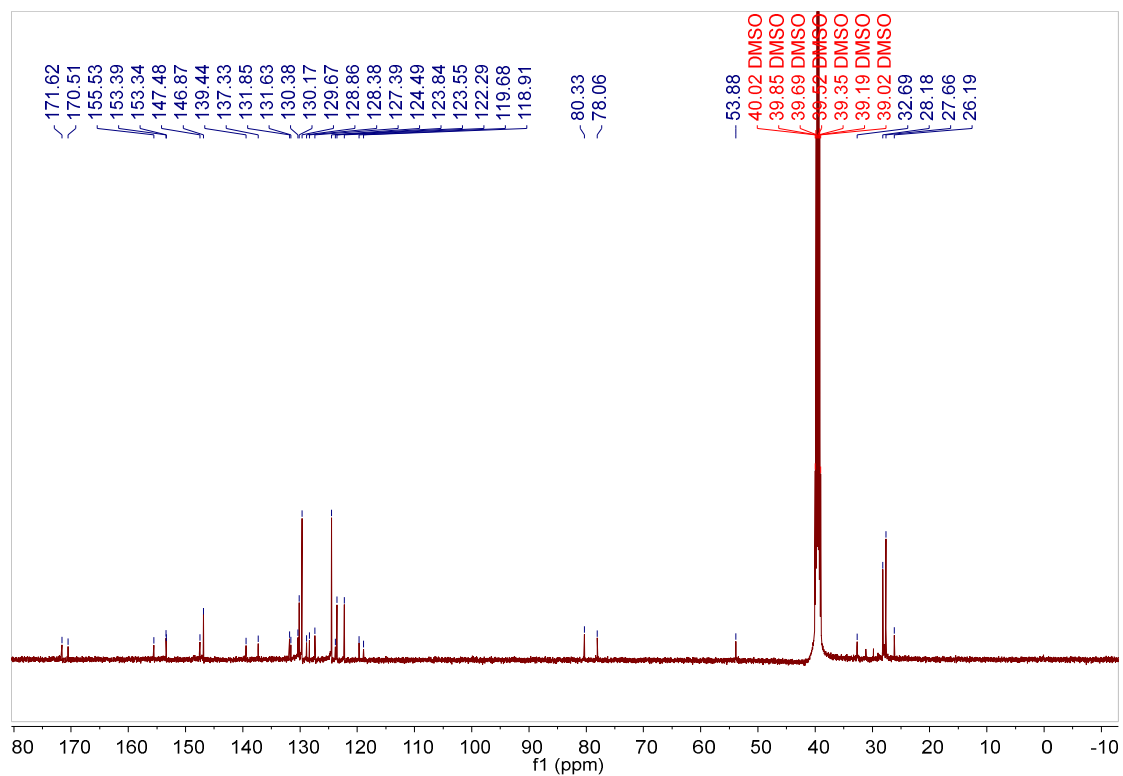
Supplementary Fig. 7. ¹³C NMR spectrum of TBpA.



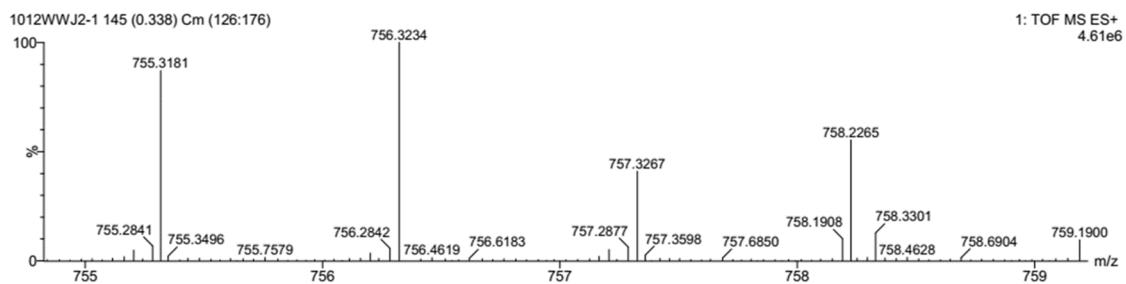
Supplementary Fig. 8. HRMS spectrum of **5a**.



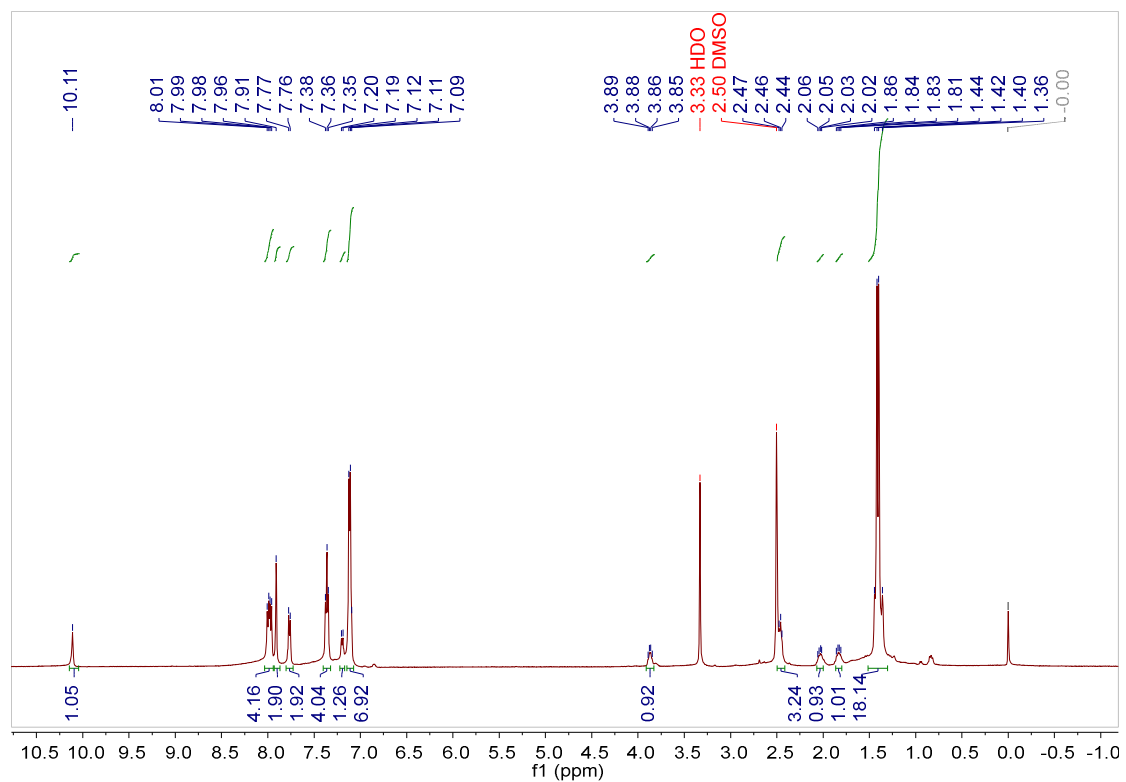
Supplementary Fig. 9. ¹H NMR spectrum of **5a**.



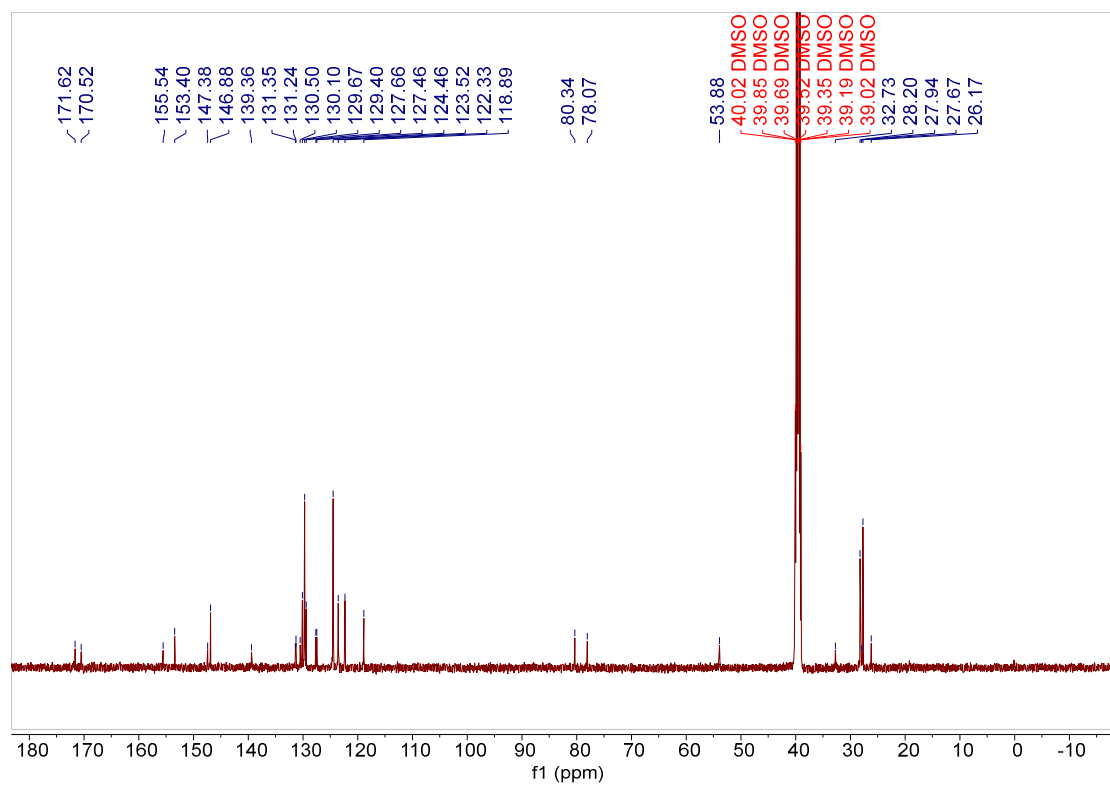
Supplementary Fig. 10. ¹³C NMR spectrum of 5a.



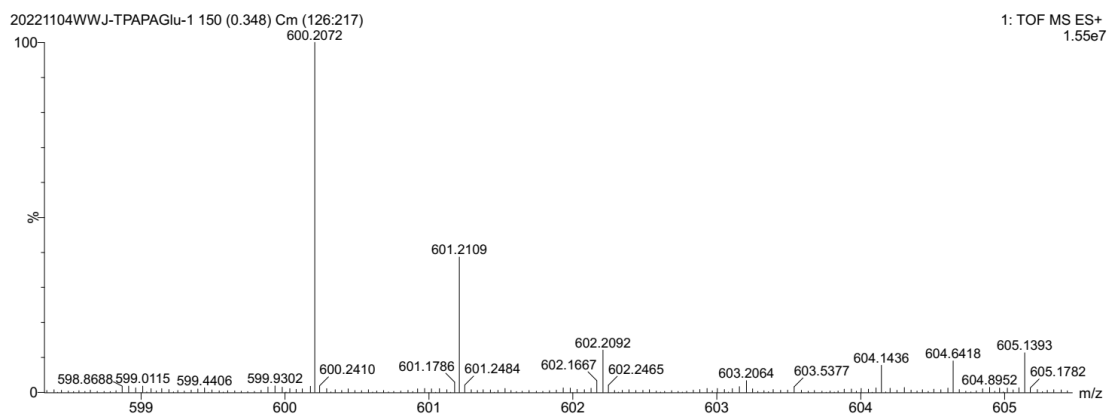
Supplementary Fig. 11. HRMS spectrum of 5b.



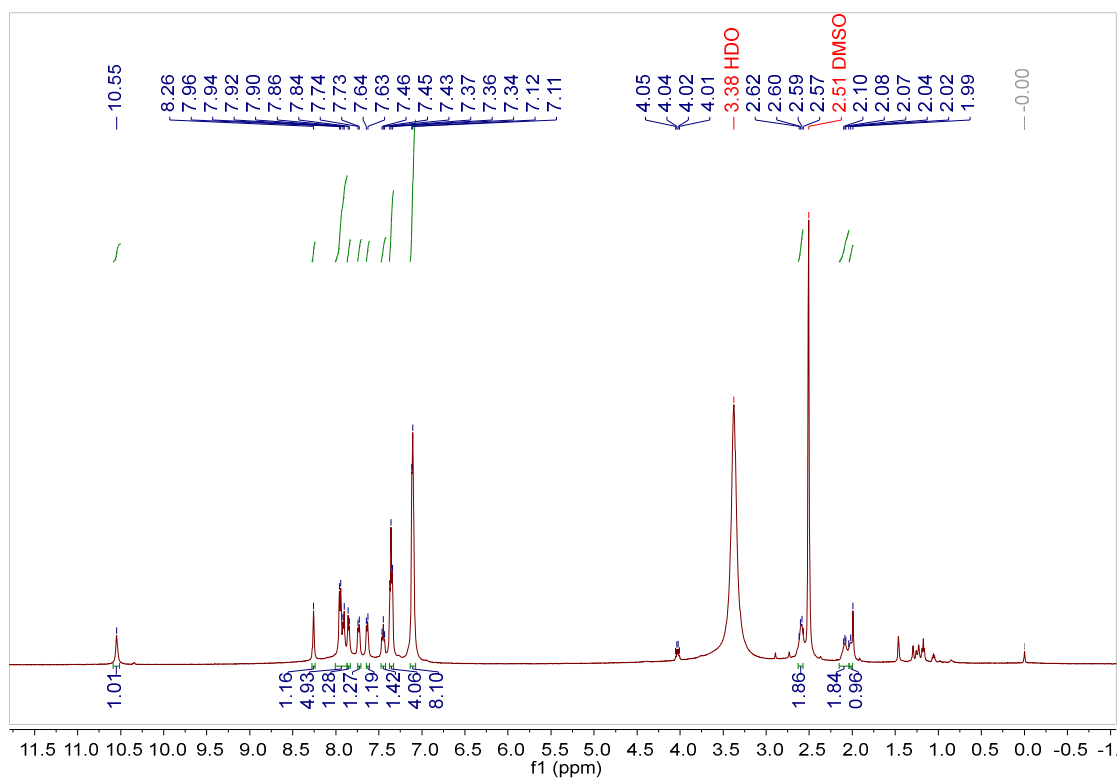
Supplementary Fig. 12. ^1H NMR spectrum of **5b**.



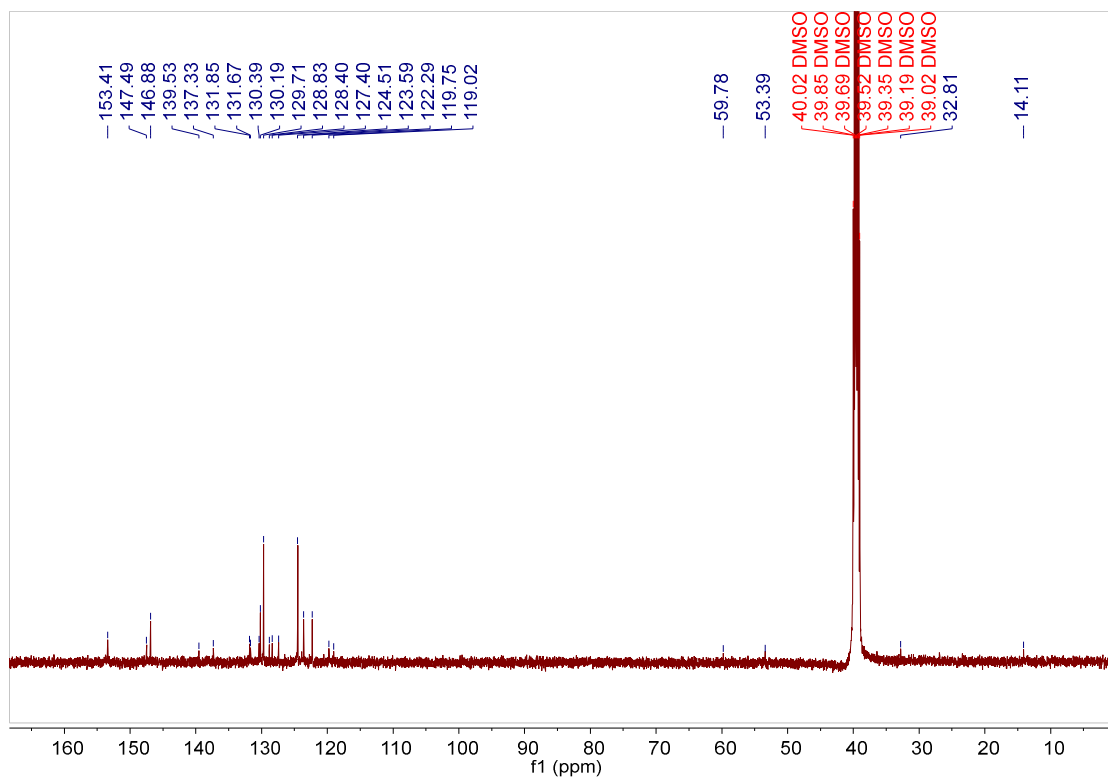
Supplementary Fig. 13. ^{13}C NMR spectrum of **5b**.



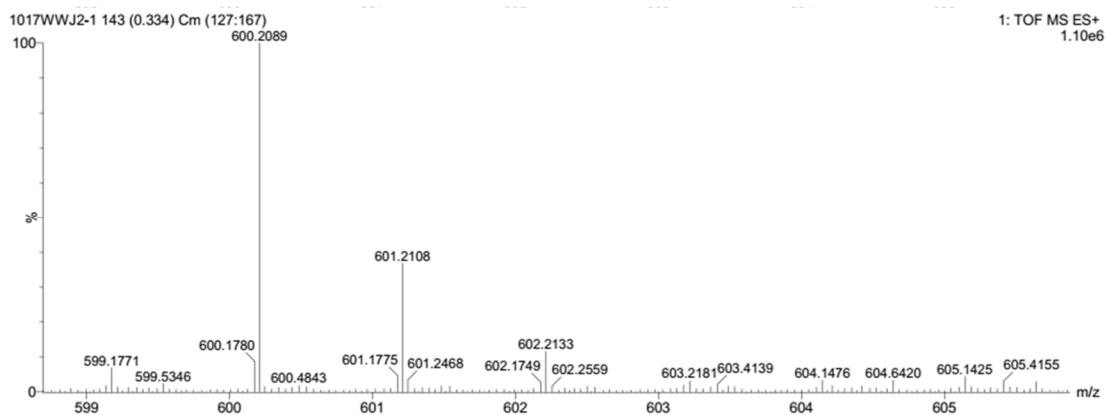
Supplementary Fig. 14. HRMS spectrum of TBmA-Glu.



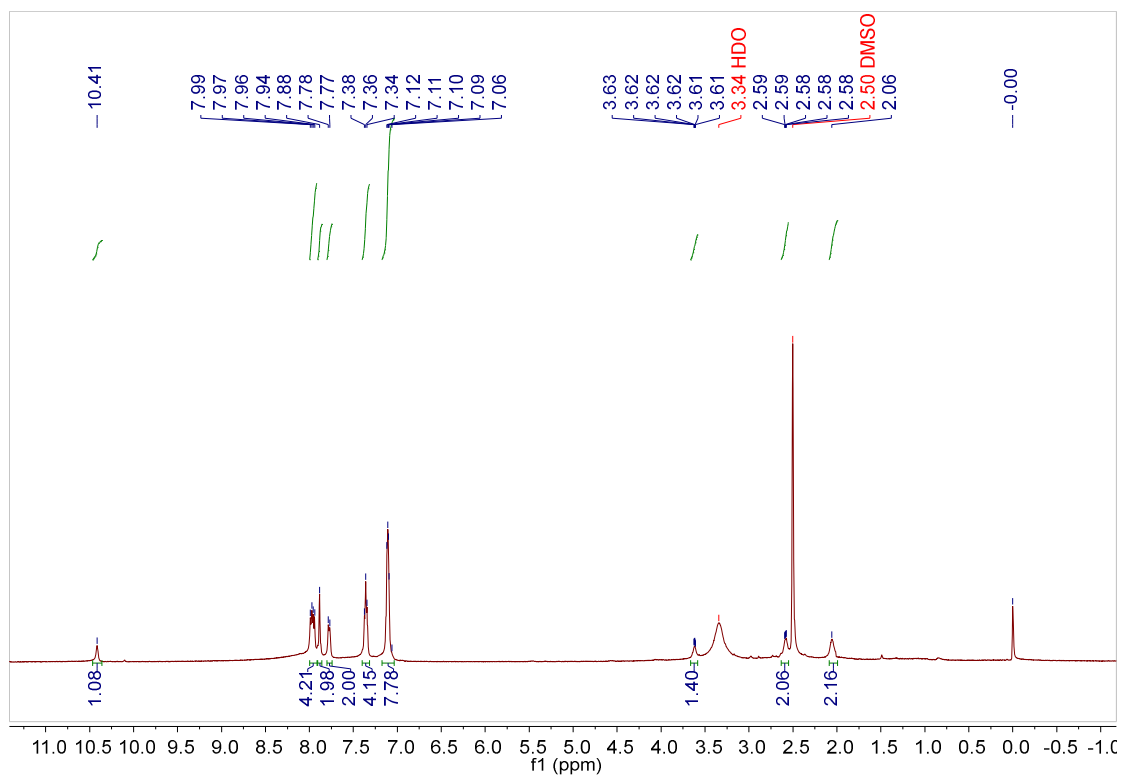
Supplementary Fig. 15. ¹H NMR spectrum of TBmA-Glu.



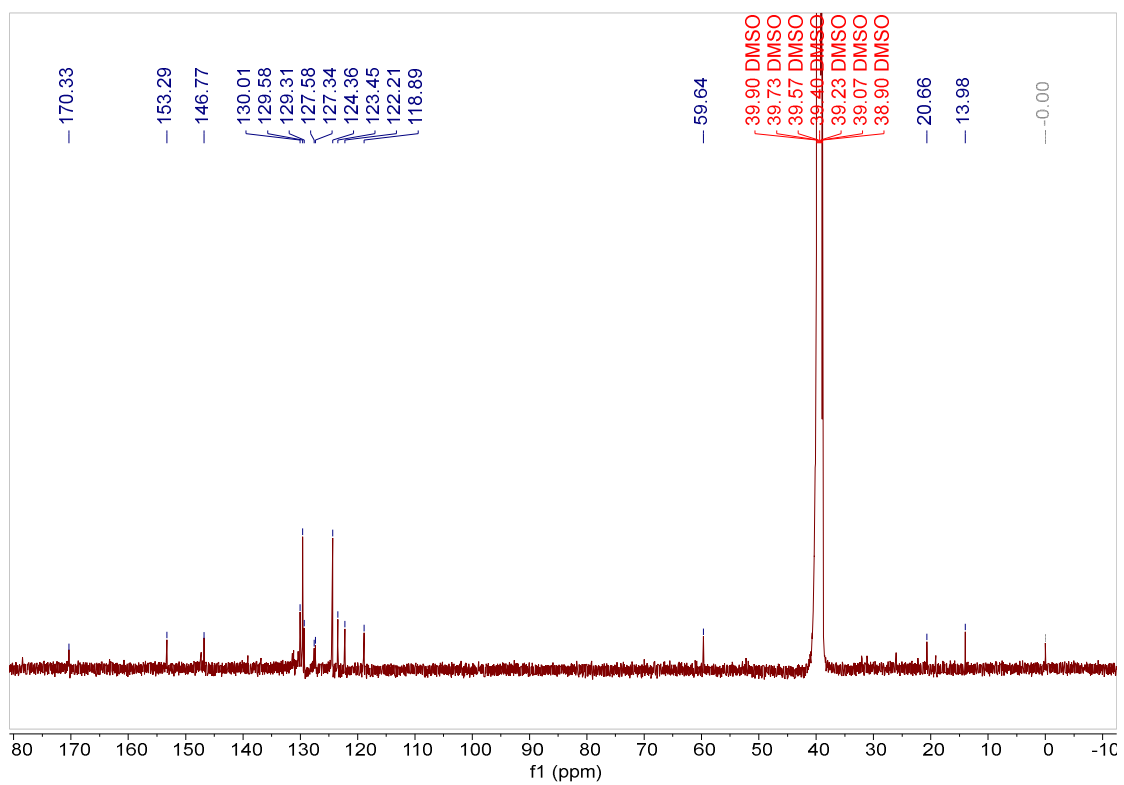
Supplementary Fig. 16. ^{13}C NMR spectrum of TBmA-Glu.



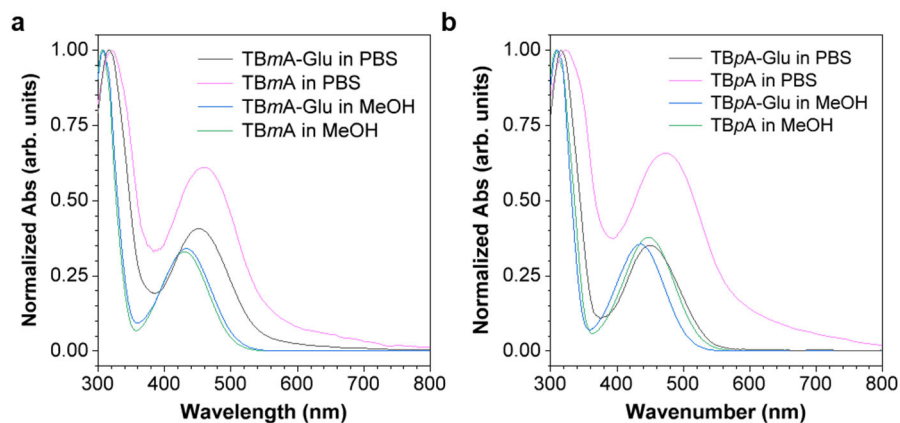
Supplementary Fig. 17. HRMS spectrum of TBpA-Glu.



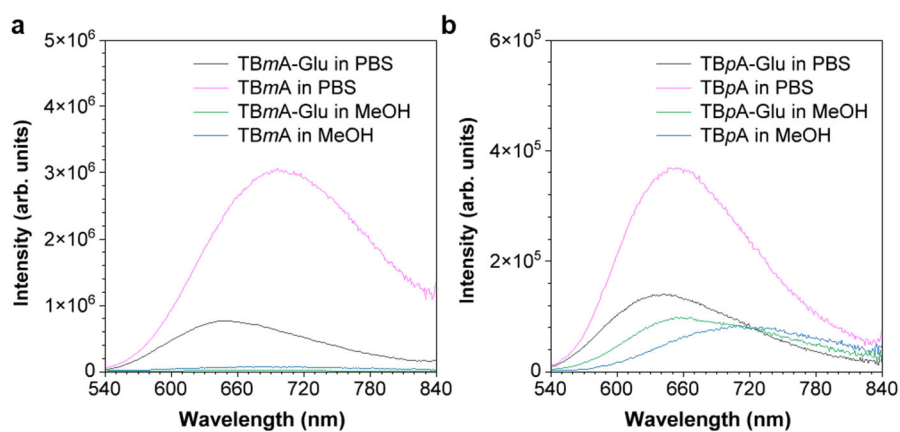
Supplementary Fig. 18. ^1H NMR spectrum of TBpA-Glu.



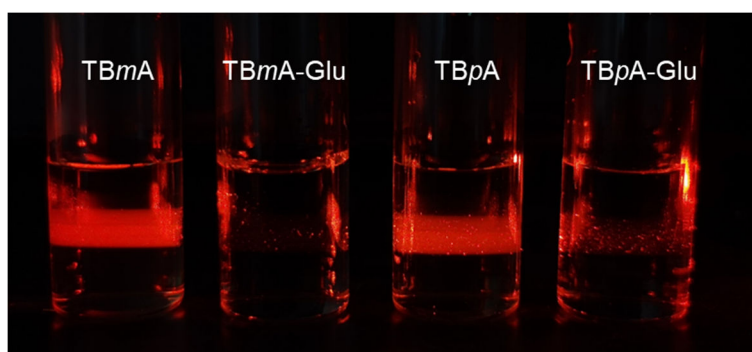
Supplementary Fig. 19. ^{13}C NMR spectrum of TBpA-Glu.



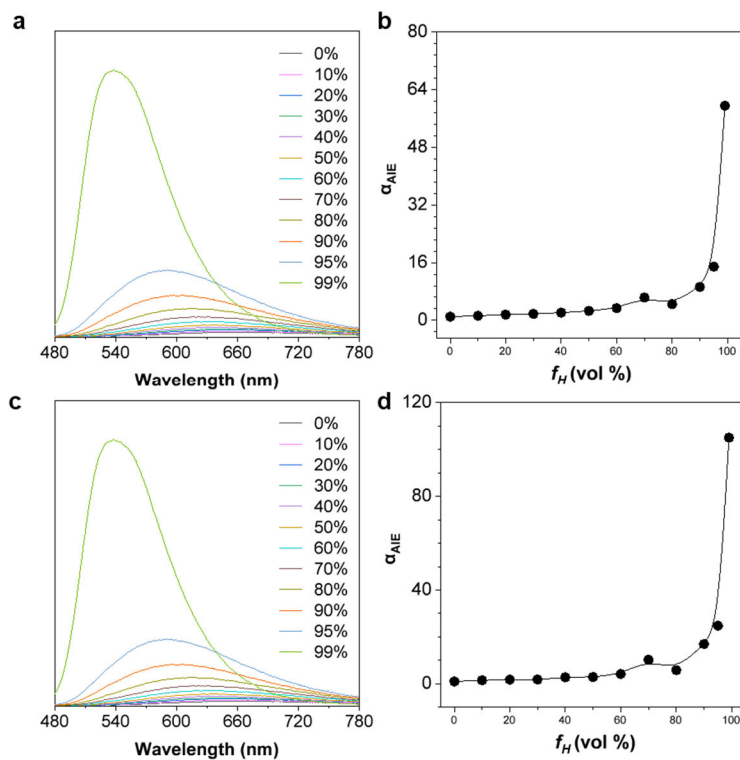
Supplementary Fig. 20. Normalized absorption spectra of (a) TBmA-Glu/TBmA and (b) TBpA-Glu/TBpA in MeOH and PBS buffer solutions ($c = 10 \mu\text{M}$).



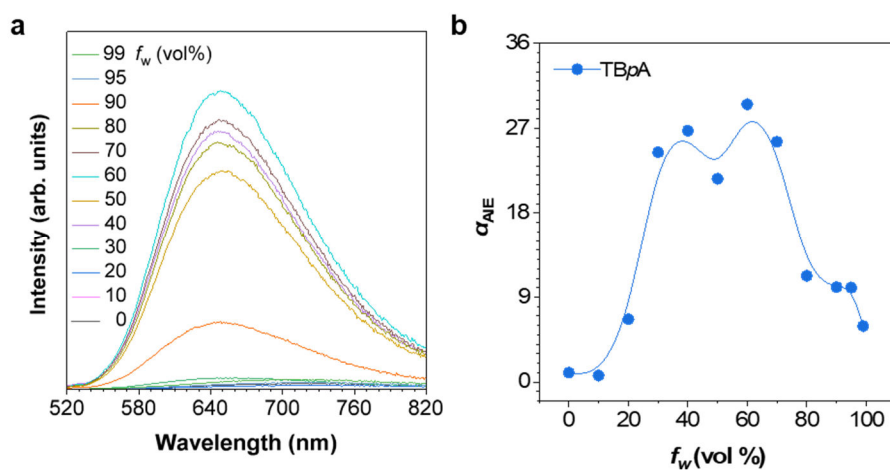
Supplementary Fig. 21. Emission spectra of (a) TBmA-Glu/TBmA and (b) TBpA-Glu/TBpA in MeOH and PBS buffer solutions ($c = 10 \mu\text{M}$), $\lambda_{\text{ex}} = 455 \text{ nm}$.



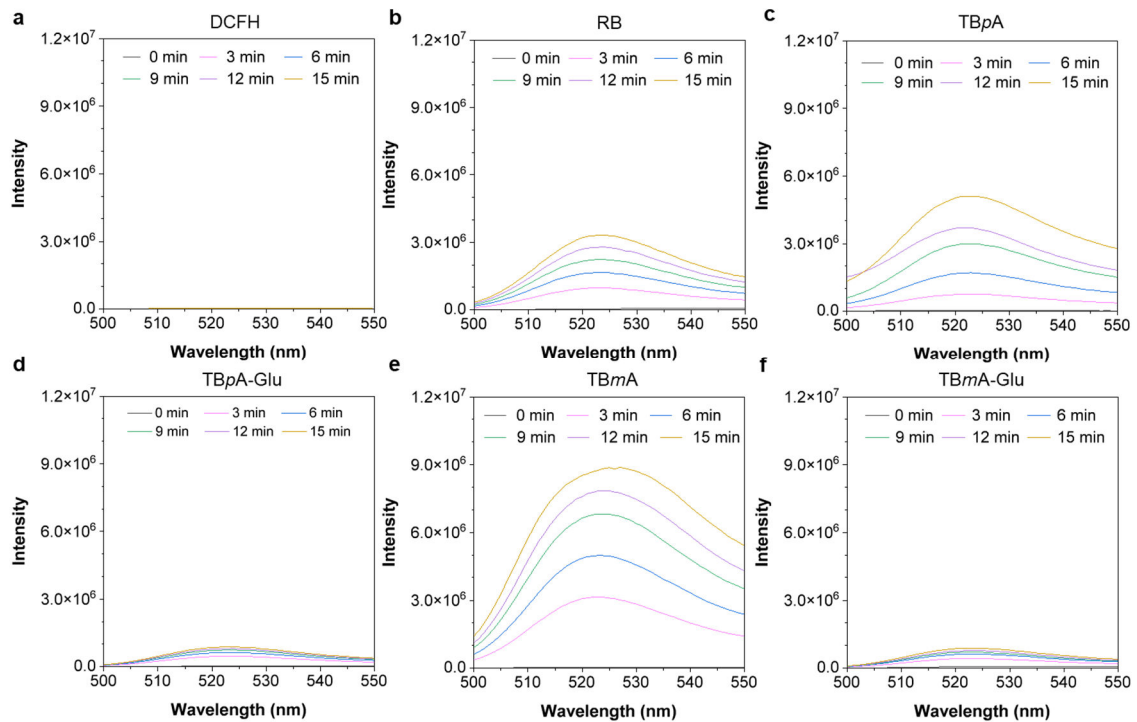
Supplementary Fig. 22. The Tyndall effect of the TBmA, TBmA-Glu, TBpA and TBpA-Glu solution was irradiated by a red laser.



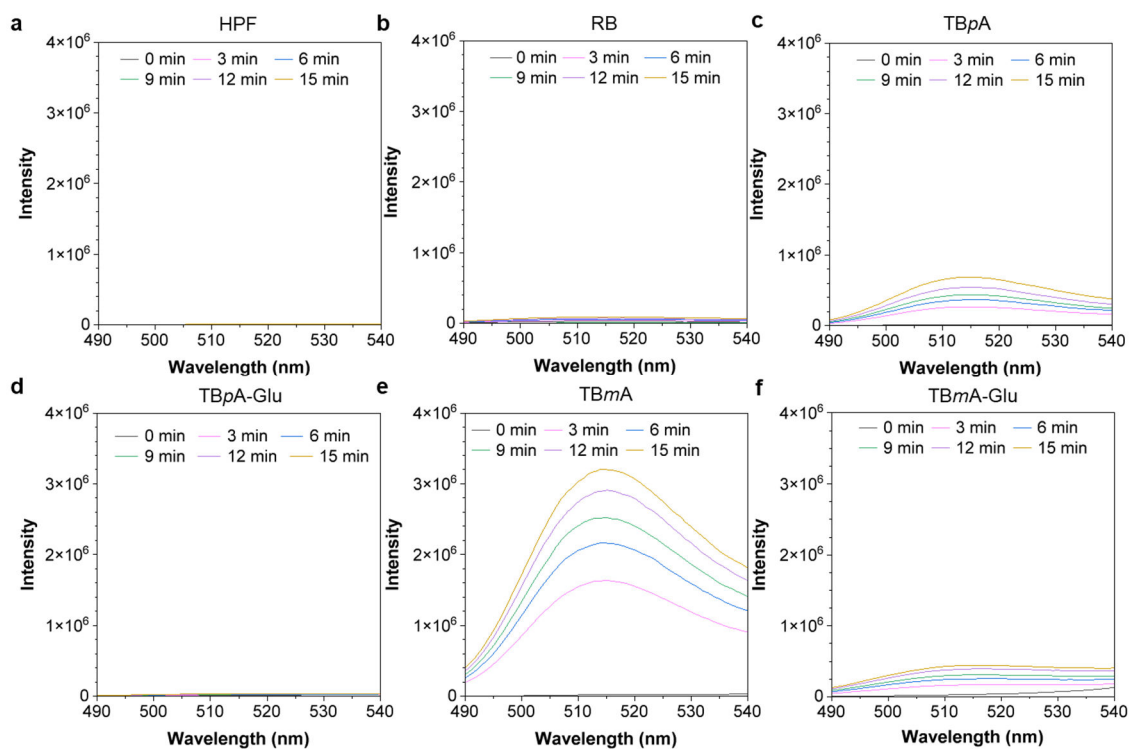
Supplementary Fig. 23. Emission spectra of TBmA-Glu (a, 10 μ M) and TBpA-Glu (c, 10 μ M) in MeOH/n-Hexane mixtures with different n-hexane fractions (f_H). The plot of I/I_0 of TBmA-Glu (b) and TBpA-Glu (d) versus f_H , where I_0 = PL intensity in pure MeOH. λ_{ex} = 455 nm.



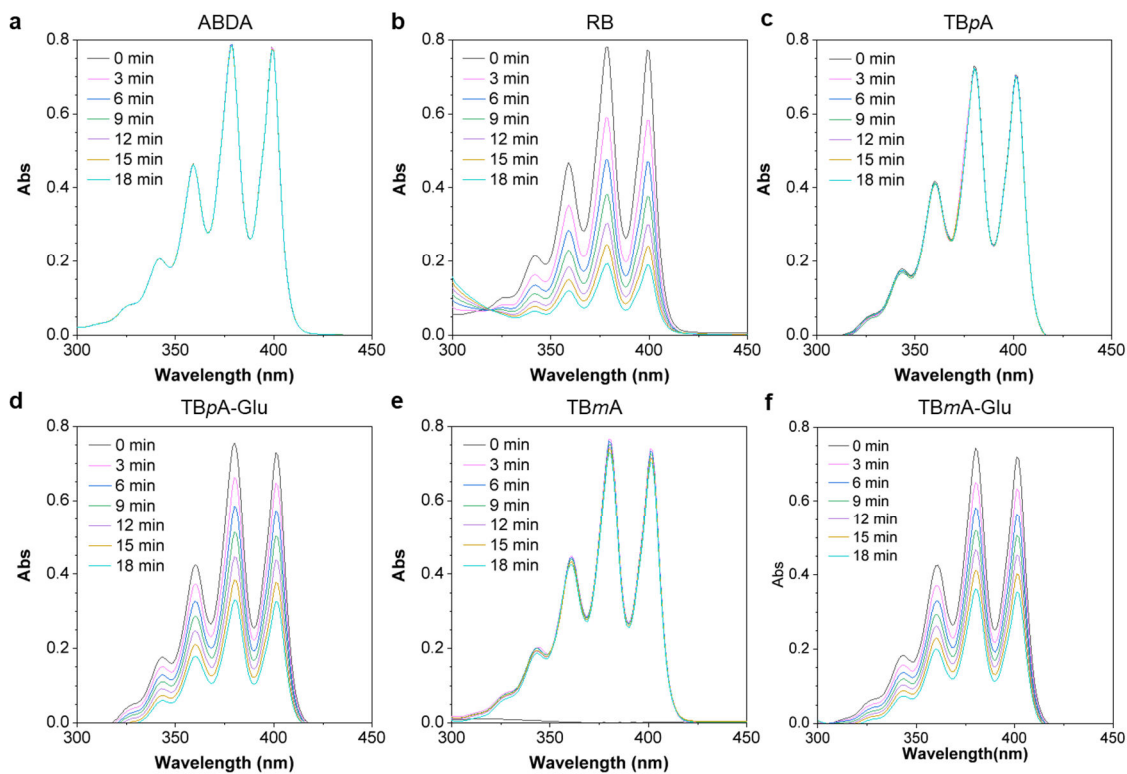
Supplementary Fig. 24. (a) Emission spectra of 10 μ M TBpA in DMF/water mixtures with different water fractions (f_w). λ_{ex} = 455 nm; (b) Plot of α_{AIE} (I/I_0 , where I_0 = PL intensity in pure DMF) of TBpA versus f_w .



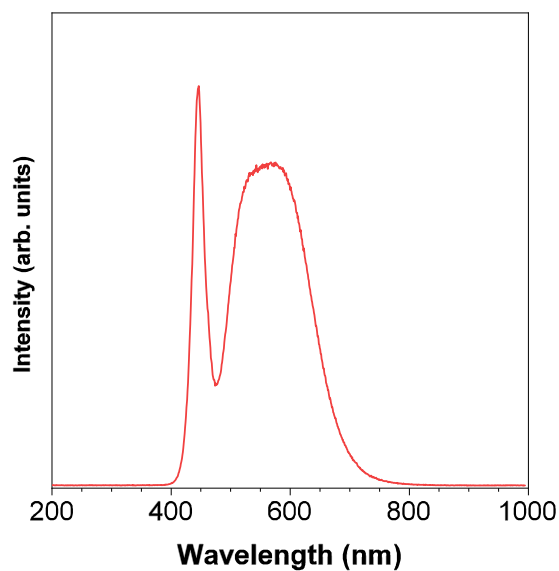
Supplementary Fig. 25. Fluorescence emission changes of DCFH (Dichlorodihydrofluorescein, 10 μM) in the presence of 5 μM photosensitizers in DMSO-PBS ($v:v = 1:99$) after irradiation ($20 \text{ mW}\cdot\text{cm}^{-2}$) for a different time. (a) DCFH, (b) Rose Bengal (RB), (c) TBpA, (d) TBpA-Glu, (e) TBmA, (f) TBmA-Glu. DCHF, $\lambda_{\text{ex}} = 488 \text{ nm}$.



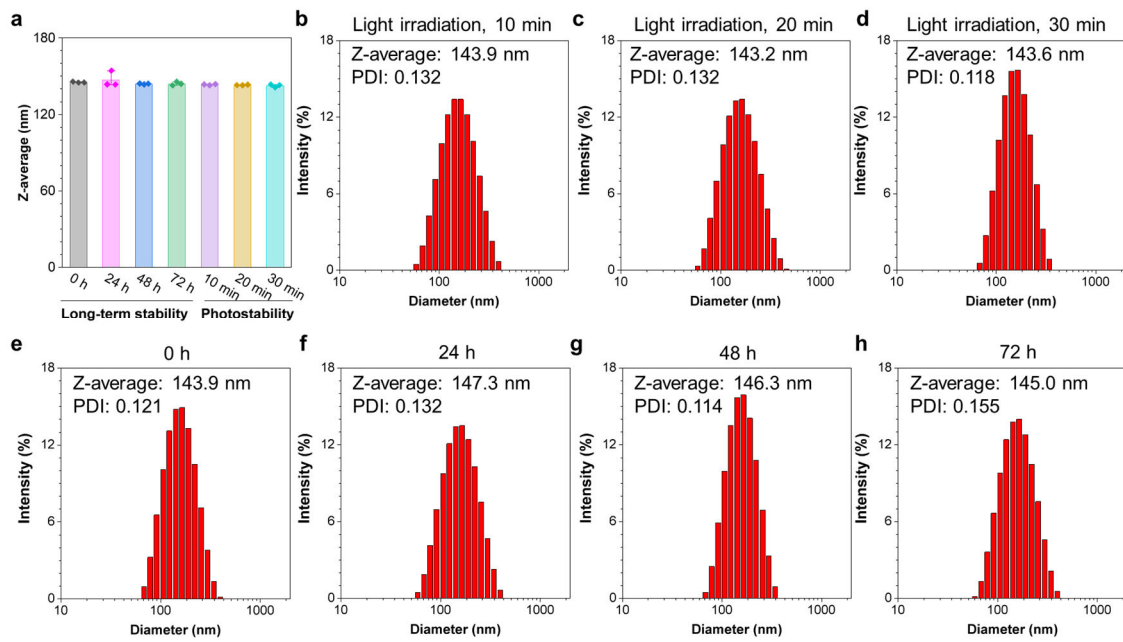
Supplementary Fig. 26. Fluorescence emission changes of HPF (hydroxyphenyl fluorescein, $10 \mu\text{M}$) in the presence of $5 \mu\text{M}$ photosensitizers in DMSO-PBS ($v:v = 1/99$) after irradiation ($20 \text{ mW}\cdot\text{cm}^{-2}$) for different times. (a) Control, (b) RB, (c) TBpA, (d) TBpA-Glu, (e) TBmA, (f) TBmA-Glu. HPF, $\lambda_{\text{ex}} = 488 \text{ nm}$.



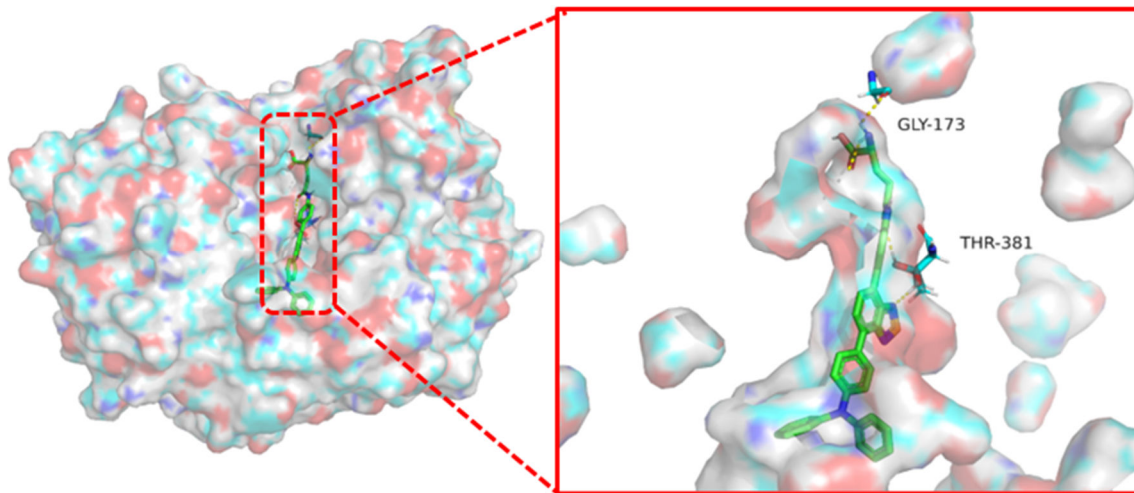
Supplementary Fig. 27. UV-vis spectra of (a) 9,10-anthracenediyl-bis(methylene)dimalonic Acid (ABDA) in the presence of (b) RB, (c) TBpA, (d) TBpA-Glu, (e) TBmA, (f) TBmA-Glu in DMSO/PBS ($v:v = 1:99$) mixture under the irradiation with different time. Concentration: 100 μM for ABDA, 5 μM for AIE photosensitizers, white light irradiation (20 mW cm^{-2}).



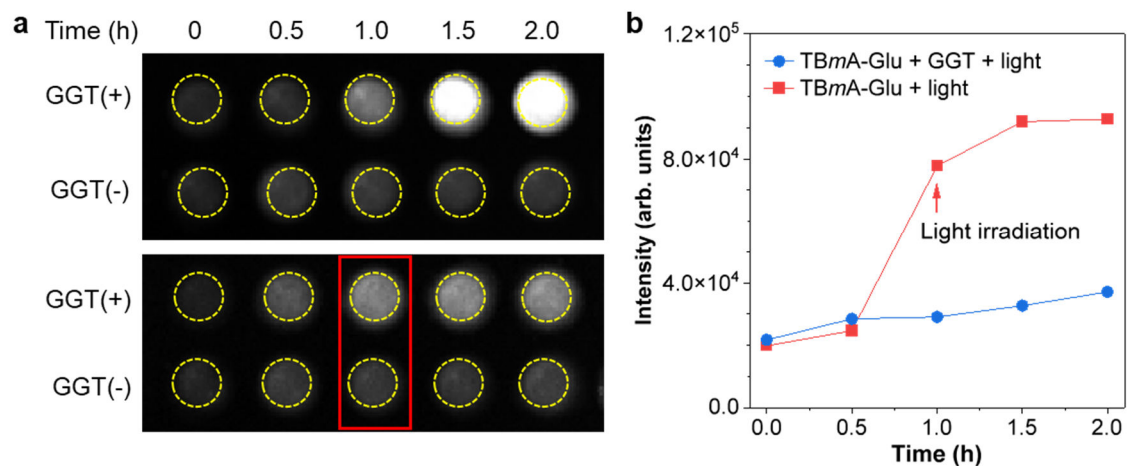
Supplementary Fig. 28. The emission wavelength analysis of the LED light.



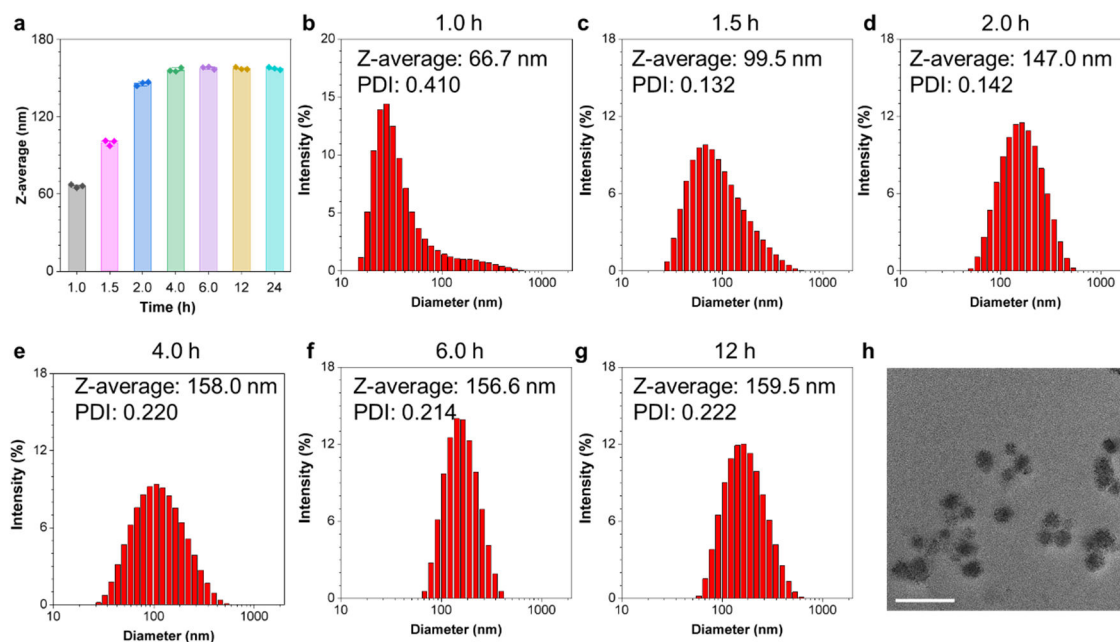
Supplementary Fig. 29. The average hydrodynamic diameters (Z-average) of TBmA aggregates are measured by Dynamic Light Scattering (DLS). The distribution of TBmA aggregates during 30 min light irradiation and 72 h FBS preservation.



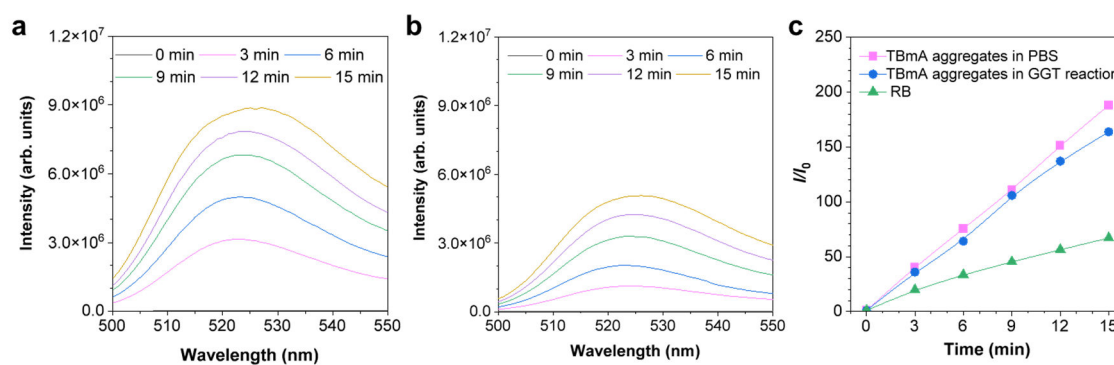
Supplementary Fig. 30. The molecular docking results of TBpA-Glu with GGT (PDB: 4GG2). The TBpA-Glu are colored green, and the molecular surface of GGT is shown as a colorful surface with transparency. The enlarged images show the hydrogen bonds formed between TBpA-Glu and γ -Glutamyltransferase (GGT).



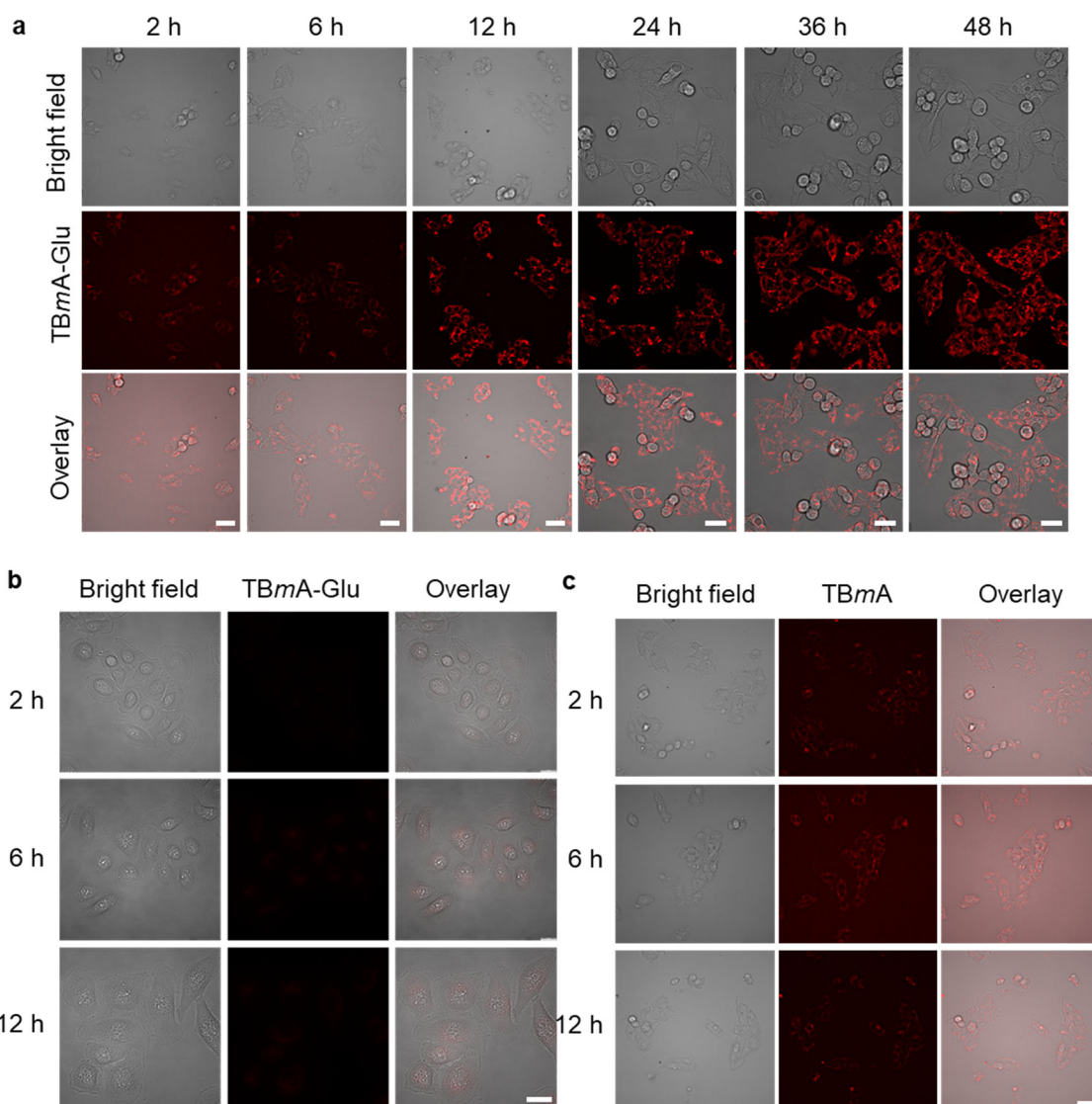
Supplementary Fig. 31. (a) The fluorescence images of TBmA-Glu in the absence or the presence of GGT. The red arrow indicates the time point for light irradiation ($12 \text{ J} \cdot \text{cm}^{-2}$). (b) Fluorescence intensity changes of TBmA-Glu incubated in the HEPES buffer at $37 \text{ }^\circ\text{C}$ in the presence and absence of GGT with a white light LED array irradiation ($12 \text{ J} \cdot \text{cm}^{-2}$). The red arrows indicate the time points for light irradiation. To a $5 \text{ } \mu\text{M}$ solution of TBmA-Glu in 10 mM HEPES buffer, $\text{pH } 7.4$, containing 0.1% DMSO as a cosolvent, 5 units of GGT was added. The reaction mixture was incubated at $37 \text{ }^\circ\text{C}$ for 1 h before the light irradiation.



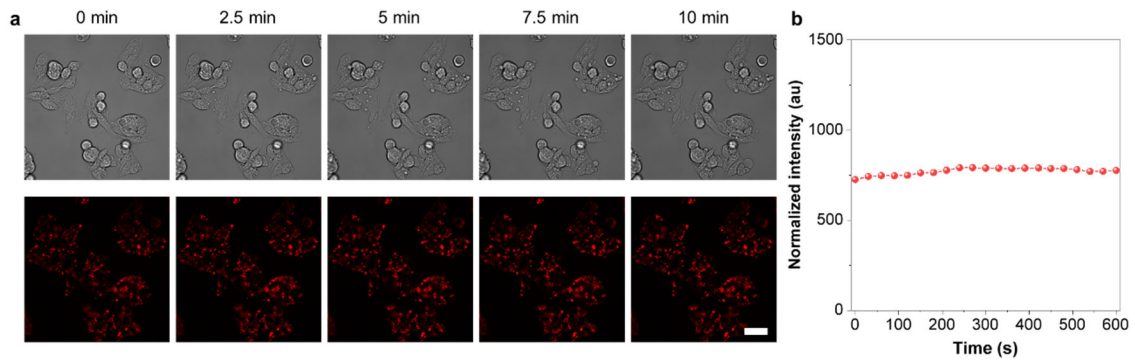
Supplementary Fig. 32. (a) The average hydrodynamic diameter (Z-average) of TBmA aggregates produced in GGT catalytic reaction measured by DLS. (b-g) Distribution of TBmA aggregates formed at different times of GGT catalytic reaction. (h) The transmission electron microscope (TEM) of the TBmA aggregates formed after the GGT catalytic reaction for 12 h.



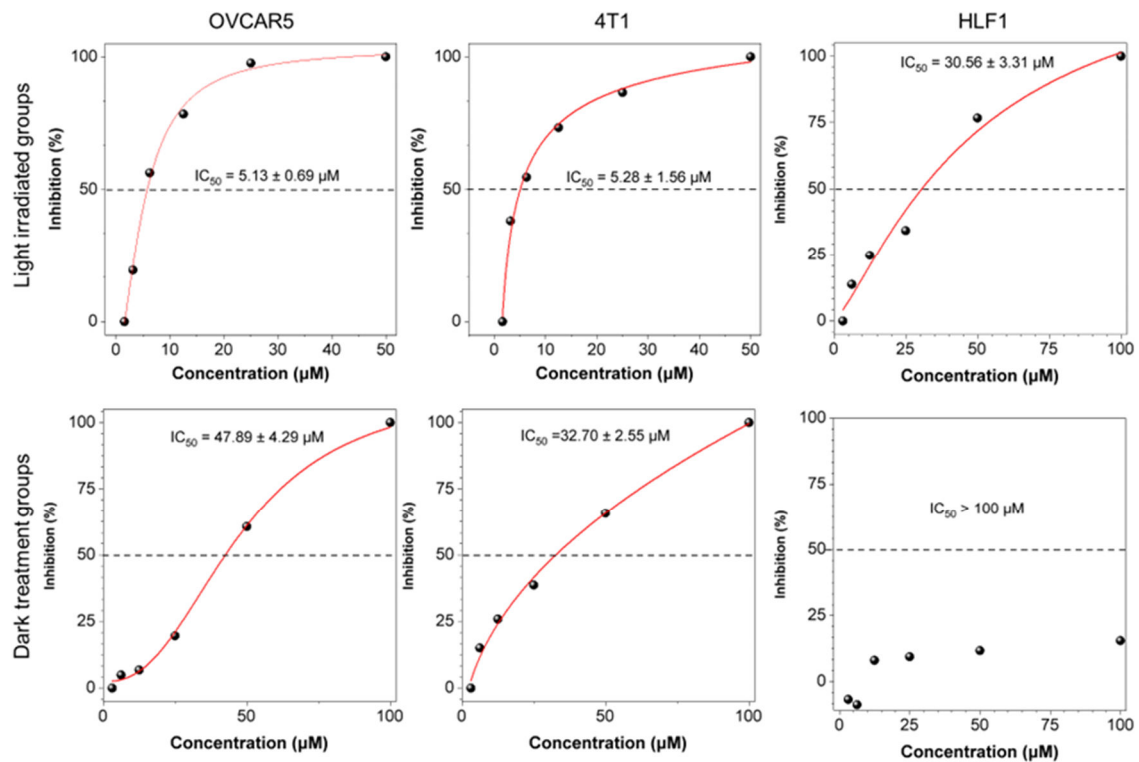
Supplementary Fig. 33. Fluorescence emission changes of DCFH (10 μM) in the presence of 5 μM photosensitizers in DMSO-PBS ($v:v=1/99$) after irradiation ($20 \text{ mW} \cdot \text{cm}^{-2}$) for different times. (a) TBmA aggregates in PBS, (b) TBmA aggregates produced in GGT catalytic reaction, DCFH, $\lambda_{\text{ex}} = 488 \text{ nm}$. (c) Plot of the relative emission intensity (I/I_0) of DCF (10 μM) in presence of TBmA (5 μM), TBmA aggregates produced in GGT reaction (5 μM) or Rose Bengal (RB, 5 μM) versus the irradiation ($20 \text{ mW} \cdot \text{cm}^{-2}$) time, where $I_0 = \text{PL intensity of DCFH in solutions with different water fraction } (f_w) \text{ without light irradiation. } \lambda_{\text{ex}} = 488 \text{ nm}$.



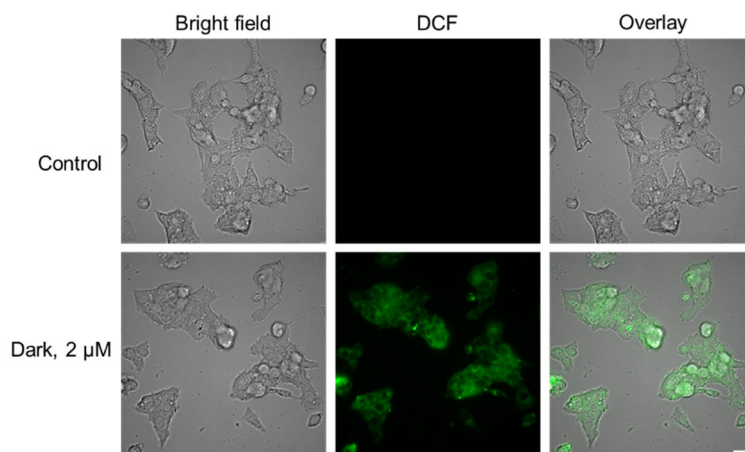
Supplementary Fig. 34. The time-dependent uptake process of TBmA-Glu (a) / TBmA (b) in HepG2 cells. (c) The time-dependent uptake process of TBmA-Glu in LO2 cells. All the cells were incubated with 5 μ M TBmA-Glu / TBmA and imaged at the indicated time. $\lambda_{\text{ex}} = 465$ nm; $\lambda_{\text{em}} = 700 \pm 20$ nm, Scale bar, 20 μ m.



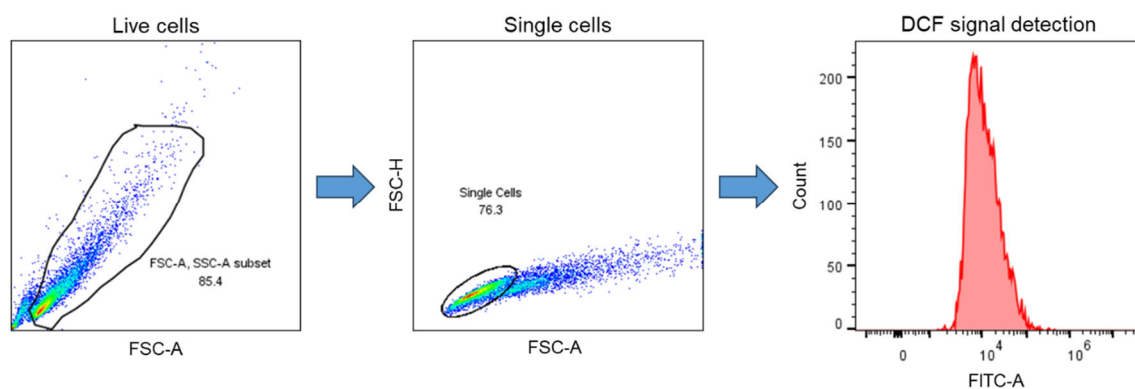
Supplementary Fig. 35. The HepG2 cells were imaged after incubation with TBmA-Glu (5 μM) for 12 hours. Subsequently, the cells were exposed to a 465 nm laser for 10 minutes, and images were captured every minute. $\lambda_{\text{ex}} = 465 \text{ nm}$; $\lambda_{\text{em}} = 700 \pm 20 \text{ nm}$, Scale bar, 20 μm .



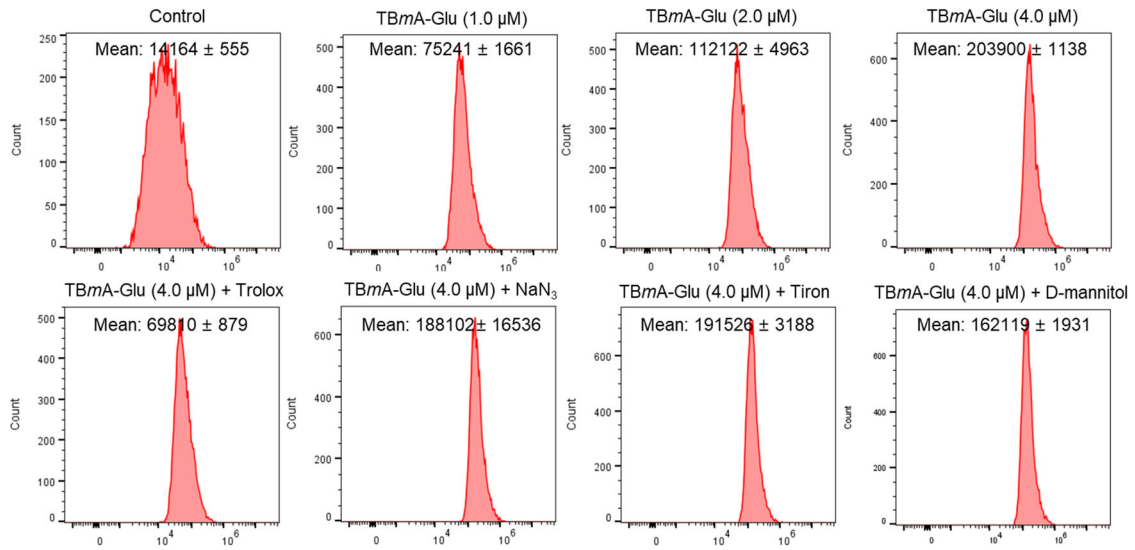
Supplementary Fig. 36. The anticancer activity (IC_{50} , μM) of TBmA-Glu against GGT overexpressing OVCAR5 and 4T1, and GGT normally expressing HLF1 cells.



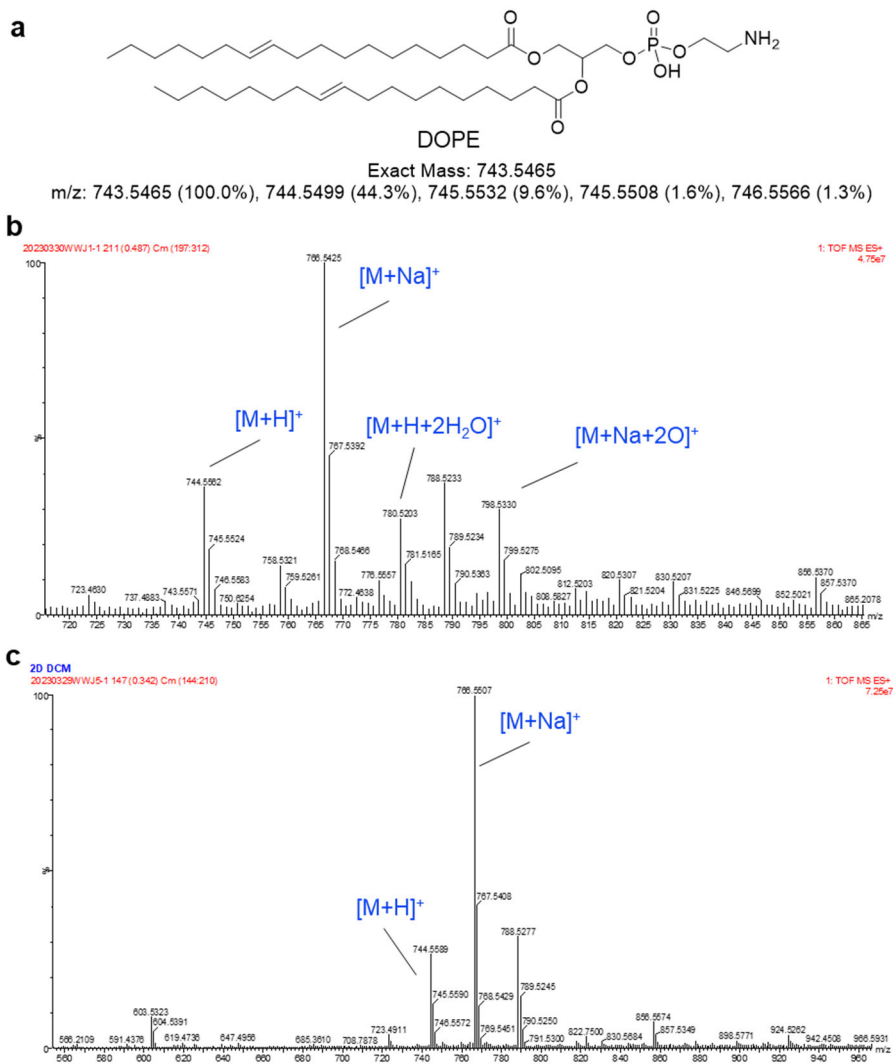
Supplementary Fig. 37. Intracellular ROS generation in HepG2 cells. HepG2 cells were incubated with TBmA-Glu (2 μ M) or 1% DMSO (Ctrl) for 24 h. DCFH-DA (10 μ M) was used as the ROS indicator. DCFH-DA, $\lambda_{\text{ex}} = 488$ nm, $\lambda_{\text{em}} = 500 \pm 20$ nm; TBmA-Glu, $\lambda_{\text{ex}} = 465$ nm, $\lambda_{\text{em}} = 700 \pm 20$ nm. Scale bar = 20 μ m.



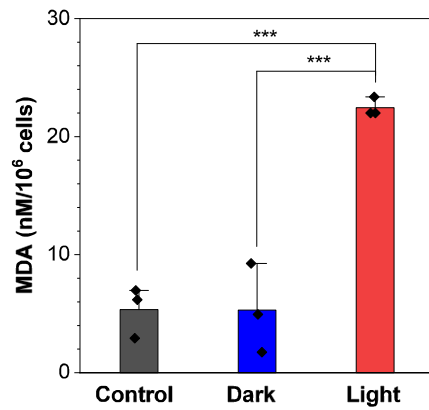
Supplementary Fig. 38. The gate strategies for flow cytometer assays.



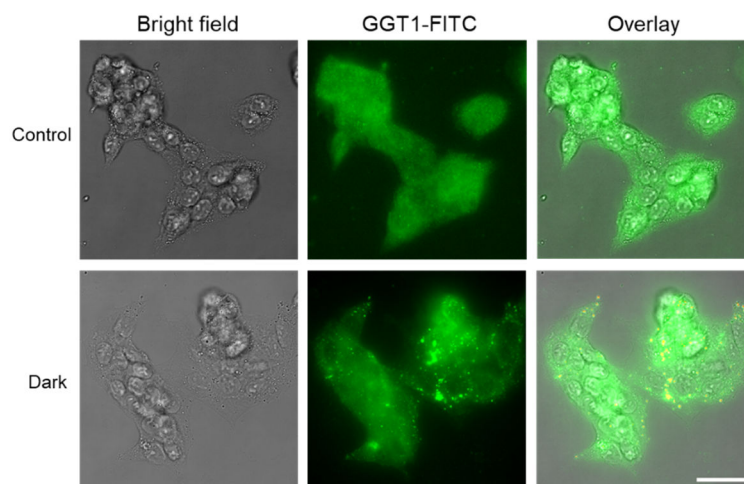
Supplementary Fig. 39. Intracellular ROS levels measured by DCF staining with flow cytometry ($\lambda_{\text{ex}} = 488 \text{ nm}$, $\lambda_{\text{em}} = 525 \pm 20 \text{ nm}$). HephG2 cells were treated with the TBmA-Glu as the indicated concentrations for 12 h and irradiated with a white laser array ($12 \text{ J}\cdot\text{cm}^{-2}$) before incubated with DCFH-DA ($10 \mu\text{M}$, 15 min). For the scavenger assay, cells were pre-incubated with the ROS scavengers for 2 h (Tiron: 10 mM; NaN_3 : 5 mM; mannitol: 50 mM; Ebselen: 50 μM), and then the cells were treated with TBmA-Glu ($4 \mu\text{M}$) for 12 h and irradiated with a white laser array ($12 \text{ J}\cdot\text{cm}^{-2}$) before incubated with DCFH-DA ($10 \mu\text{M}$, 15 min).



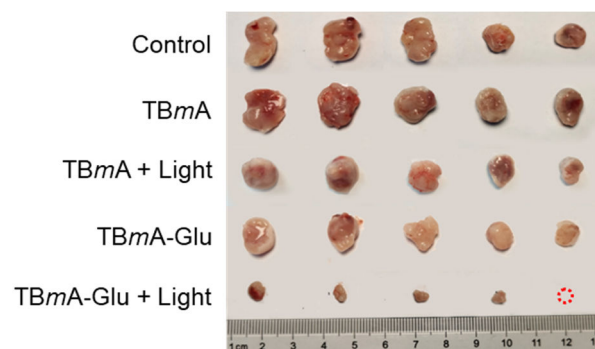
Supplementary Fig. 40. (a) The structure of 1,2-Dioleoyl-*sn*-glycero-3-phosphoethanolamine (DOPE). The results of HR-MS of DOPE (10 μ M) coincubate with TBmA (10 μ M) with (b) /without (c) light irradiation.



Supplementary Fig. 41. Malondialdehyde (MDA) levels in HepG2 cells after treated with the TBmA-Glu (2 μ M) for 12 h. Then, the cells were irradiated with a white laser array (12 J·cm⁻²) and the MDA levels were detected using a Lipid Peroxidation MDA Assay Kit. Data expressed as average \pm standard error, n = 3. Statistical significance: P values, ***P < 0.001, calculated with the one-side Student's T-test.

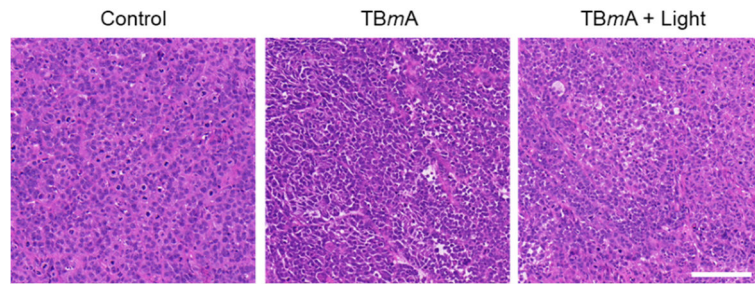


Supplementary Fig. 42. The intracellular level changes of GGT in HepG2 cells after being treated with TBmA-Glu (2 μ M) for 24 h. Scale bar, 20 μ m.

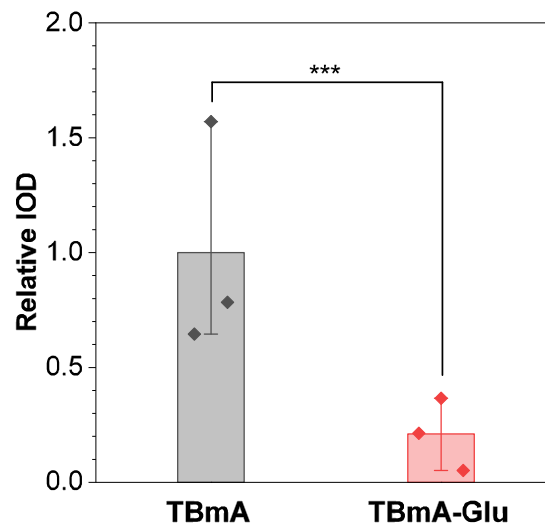


Supplementary Fig. 43. The photographs of the separated tumors in different treatment groups

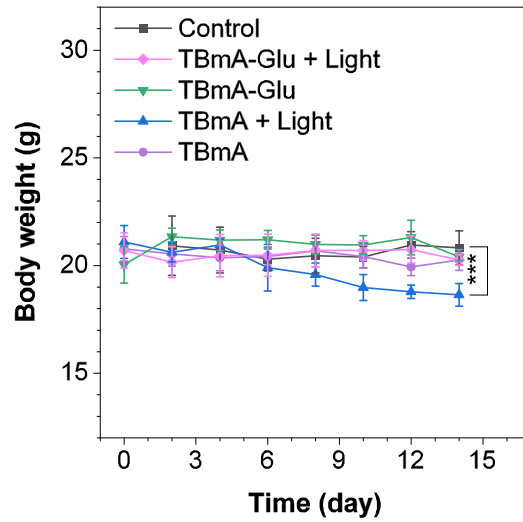
at the end of the treatment process.



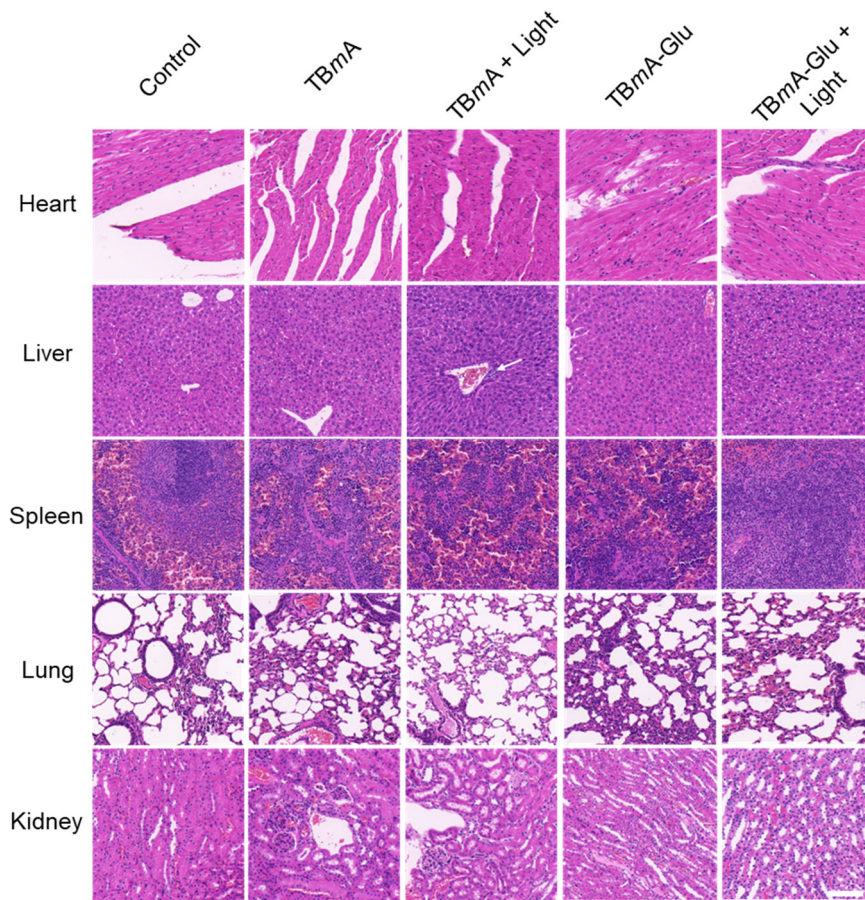
Supplementary Fig. 44. Hematoxylin-eosin staining in tumor sections from mice with different treatments. The mice were treated with TBmA (5 mg/kg) or physiological saline (Control): scale bar, 100 μ m.



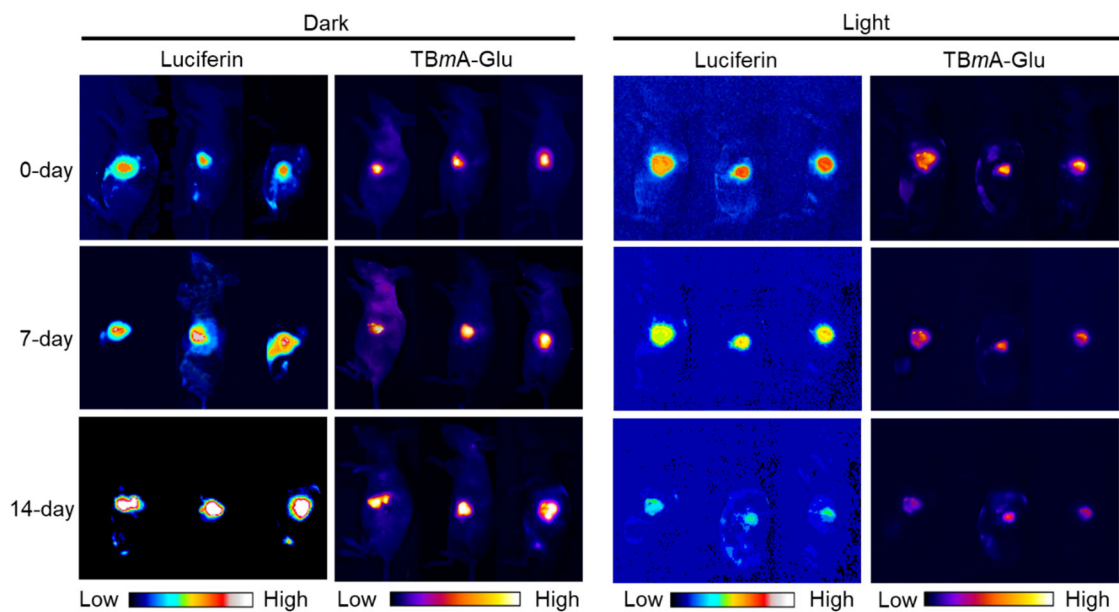
Supplementary Fig. 45. The relative integral optical density (IOD) of GPX4 in immunohistochemistry images of TBmA-Glu/TBmA (5 mg/kg) PDT groups. Data expressed as average \pm standard error, $n = 3$. Statistical significance: P values, *** $P < 0.001$, calculated with the one-sided Student's T-test.



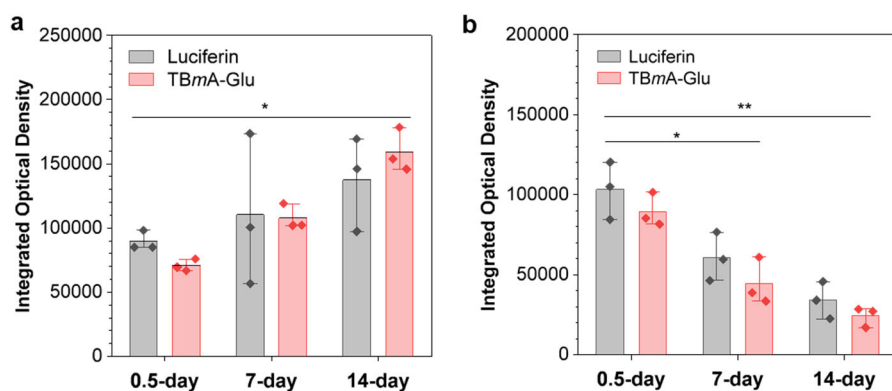
Supplementary Fig. 46. The average weight of mice after treatment with TBmA-Glu/TBmA (5 mg/kg) or physiological saline (Control). Data expressed as average \pm standard error, $n = 5$. Statistical significance: P values, *** $P < 0.001$, calculated with the one-sided Student's T-test.



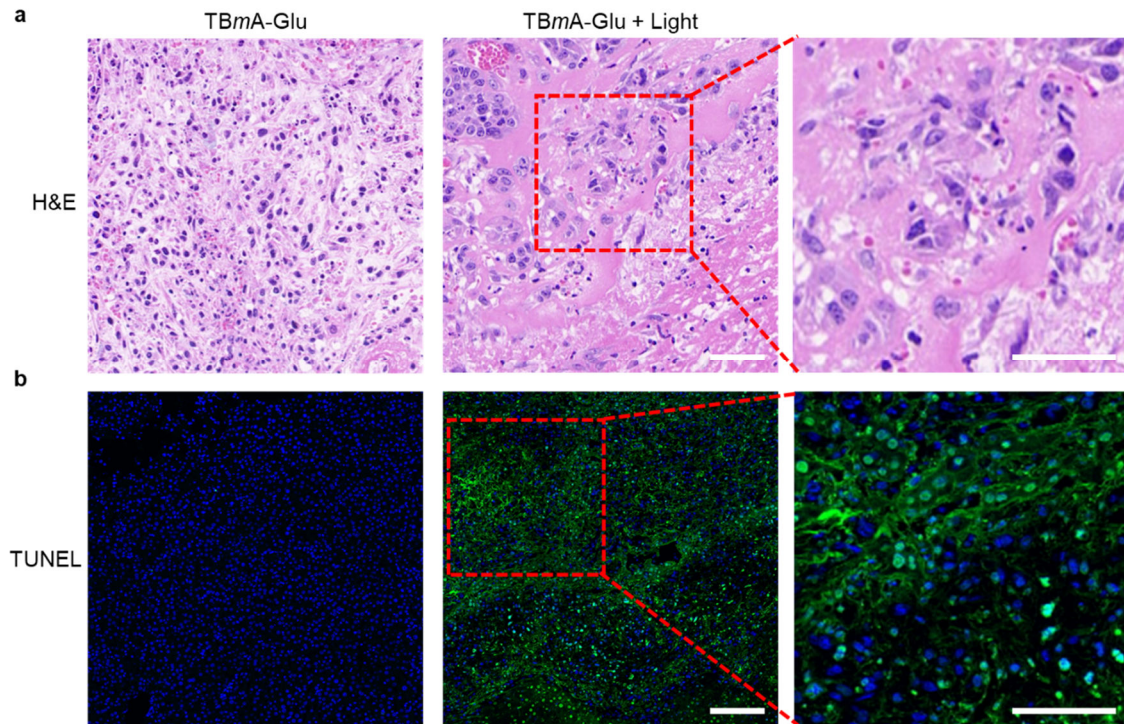
Supplementary Fig. 47. The representative hematoxylin-eosin staining images of organs from mice after treatment with TBmA-Glu/TBmA (5 mg/kg) or physiological saline (Control). Scale bar, 100 μ m.



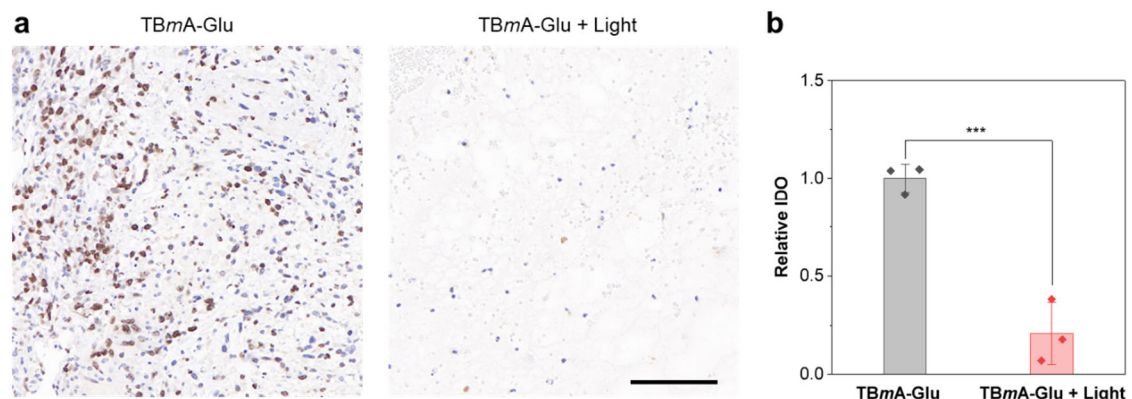
Supplementary Fig. 48. The fluorescence images of the in-situ hepatoma mice at the start, middle, and end of the treatment process by TBmA-Glu (5 mg/kg). Luminescence, $\lambda_{em} = 550 \pm 50$ nm (BP), 1000 ms. TBmA-Glu, $\lambda_{ex} = 500$ nm, $\lambda_{em} = 700$ nm (Long pass filter).



Supplementary Fig. 49. The IOD of cancer in the mice of in-situ hepatoma models after treated TBmA-Glu (5 mg/kg) without (a) or with (b) light irradiation. Data expressed as average \pm standard error, n = 3. Statistical significance: P values, *P < 0.05, **P < 0.01, calculated with the one-sided Student's T-test.



Supplementary Fig. 50. (a) The representative hematoxylin-eosin staining images of livers of the mice in an in situ hepatoma model after treatment with TBmA-Glu (5 mg/kg). The enlarged area shows fibrosis of tumor tissue after photodynamic therapy by TBmA-Glu. (b) TUNEL assay of livers of the mice in an in situ hepatoma model after treatment with TBmA-Glu (5 mg/kg). Scale bar, 100 μm and 50 μm (for the enlarged images).



Supplementary Fig. 51. (a) Ki67 staining of tumor tissue from livers of the mice in an in situ hepatoma model after being treated by TBmA-Glu (5 mg/kg). Scale =100 mm Scale bar, 100 μm . (b) The relative IOD of Ki67 in immunohistochemistry images of TBmA-Glu/TBmA-Glu (5 mg/kg) PDT groups. Data expressed as average \pm standard error, $n = 3$. Statistical significance: P values, ***P < 0.001, calculated with the one-sided Student's T-test.

Supplementary Tables

Supplementary Table S1. The results of docking with GGT.

Compounds	Ki (μM)	Intermolecular energy (Kcal/mol)	Binding energy (Kcal/mol)	Interacting amino acid residues
Glutamate	14.68	-8.37	-6.29	THR ³⁸¹ , ASN ⁴⁰¹ , ASP ⁴²³ , SER ⁴⁵¹ , SER ⁴⁵² GLY ⁴⁷³ , GLY ⁴⁷⁴
TB <i>m</i> A-Glu	0.17	-12.85	-9.27	AGR ³²⁷ , ASP ⁴²² , PHE ⁴²⁴ , ASN ⁴³¹
TB <i>p</i> A-Glu	2.86	-11.14	-7.56	GLY ¹⁷³ , THR ³⁸¹

Supplementary Table S2. The photocytotoxicity (IC_{50} , μM) of GGT activable AIE photosensitizer in different cell lines.

Compound	HepG2			HeLa			LO2		
	(GGT highly expressed)			(GGT moderately expressed)			(GGT low expressed)		
	Dark ^[a]	Light ^[b]	PI ^[c]	Dark	Light	PI	Dark	Light	PI
TBpA	28.35 ±	20.54 ±	1.38	28.47 ±	25.91 ±	1.86	24.14 ±	25.36 ±	1.19
	5.21	1.14		3.35	3.42		4.22	1.87	
TBpA-Glu	23.51 ±	6.70 ±	3.51	20.31 ±	15.24 ±	1.98	53.45 ±	30.14 ±	1.77
	2.31	0.21		2.24	1.10		3.51	1.28	
TBmA	25.22 ±	12.54 ±	2.01	21.46 ±	26.36 ±	1.19	25.49 ±	28.58 ±	1.14
	2.40	2.24		4.85	2.25		3.47	2.27	
TBmA-Glu	20.12 ±	2.15 ±	9.36	33.22 ±	10.53 ±	3.15	47.17 ±	40.45 ±	1.17
	3.74	0.23		2.66	3.67		5.81	1.54	

[a] Cells were incubated with the tested compounds for 24 h and detected by MTT assay; [b] Cells were incubated with the compounds in the dark for 24 h. The light treatment groups were irradiated with a white led array ($12 J \cdot cm^{-2}$) after incubation for 12 h, then incubated for another 12 h. [c] Phototoxicity index (PI) is defined as the ratio of $^{dark}IC_{50} / ^{light}IC_{50}$.

Supplementary References

1. Liu S, Zhang H, Li Y, Liu J, Du L, Chen M, *et al.* Strategies to enhance the photosensitization: polymerization and the donor-acceptor even-odd effect. *Angew. Chem. Int. Ed.* **57**, 15189-15193 (2018).